ORIGINAL ARTICLE

# Majoon Chobchini attenuates arthritis disease severity and RANKL-mediated osteoclastogenesis in rheumatoid arthritis

Snigdha Samarpita[1] · Hari Madhuri Doss[1] · Ramamoorthi Ganesan[1,2] · Mahaboobkhan Rasool[1]

## Abstract

Majoon Chobchini, a polyherbal Unani compound, has been used holistically in India to treat rheumatoid arthritis. However, the potential mechanism underlying the antiarthritic efficacy of Majoon Chobchini has not been elucidated so far. This study was aimed to explore the underlying molecular mechanism and scientifically validate the therapeutic basis of Majoon Chobchini in rheumatoid arthritis (RA). The anti-arthritic efficacy of Majoon Chobchini was demonstrated in vivo using complete Freund's adjuvant-induced arthritic rat model and adjuvant-induced arthritic fibroblast-like synoviocytes (AA-FLS). The expression of pro-inflammatory mediators and enzymes was evaluated in the serum and synovial tissues of adjuvant-induced arthritis (AIA) rats. In-vitro, AA-FLS, and bone marrow macrophages (BMMs) were co-cultured to evaluate the formation and activity of osteoclasts using TRAP staining analysis and pit formation assay, respectively. RANKL and OPG levels were detected using western blotting and qRT-PCR analysis. Furthermore, the involvement of JAK-STAT-3 signaling in the therapeutic efficacy of Majoon Chobchini was evaluated both in vivo and in vitro. Majoon Chobchini significantly reversed the physical symptoms in AIA rats with reduced expression of pro-inflammatory cytokines and enzymes. Notably, Majoon Chobchini alleviated cartilage degradation and bone erosion in AIA rats via inhibiting the activation of the JAK-STAT-3 signaling pathway in the AIA rats. Consistent with its effect in vivo, Majoon Chobchini decreased osteoclast inducing potential of AA-FLS and thus attenuated osteoclast formation and bone resorption in vitro. Taken together, our findings suggest that the JAK/STAT-3 signaling inhibition may underlie the mechanism through which Majoon Chobchini provides relief against RA symptoms.

**Keywords** Rheumatoid arthritis · Synovial inflammation · Cartilage damage · Osteoclastogenesis · Majoon Chobchini

## Introduction

Rheumatoid arthritis (RA) is a chronic autoimmune disorder that majorly involves diarthrodial joints. The disease progression of RA has devastating pathological consequences that include persistent inflammation and irreversible destruction of multiple joints leading to considerable disability and reduced life expectancy. It has been reported that a large number of immune cells like monocytes, neutrophils, dendritic cells, and T cells flood into the synovial compartment, thus engendering chronic inflammation in RA (Hyrich and Inman 2001). This excessive immune cell infiltration and subsequent paramount inflammatory microenvironment activate fibroblast-like synoviocyte (FLS) cells that acquire aggressive features and establish invasive synovitis (Susan and Firestein 2004). Activated FLS and infiltrating immune cells in the hyperplastic synovium, in turn, release various pro-inflammatory mediators alike tumor necrosis factor (TNF)-α, interleukin (IL)-6, IL-1β, and IL-17 that further supports the development and expansion of hyperplastic RA synovium (McInnes and Schett 2007). Excessive secretion of enzymes (COX-2 and iNOS) also worsens pathological disease manifestations of RA via damaging complex antioxidant defense systems and inducing a sustained oxidative stress environment (Jaswal and Mehta 2003). While pro-inflammatory cytokines and enzymes exert their pathogenic activities through precipitating inflammation in synovial

✉ Mahaboobkhan Rasool
mkr474@gmail.com

1  SMV 240, Immunopathology Lab, School of Biosciences and Technology, Vellore Institute of Technology (VIT), Vellore, Tamil Nadu 632 014, India

2  Present Address: Immunology Program, Department of Clinical Science, H. Lee Moffitt Cancer Center, Tampa, FL 33612, USA

tissues, they also promote osteoclastogenesis via upregulating RANKL expression. Receptor activator of nuclear factor kappa-B ligand (RANKL), an osteoimmunological molecule, is majorly secreted via RA-FLS cells and necessitates osteoclast differentiation and activation that aggravates bone erosion process in RA (Jung et al. 2014).

Currently, combinational use of disease-modifying anti-rheumatic drugs (DMARDs) and biologics is widely considered early aggressive therapy for treating and managing RA. However, these therapeutic settings develop opportunistic infections, and many patients cannot tolerate them well. Also, cytokine blockade therapies are more expensive, and the route of administration is restricted (Luo et al. 2013). Indeed, blockade of RANKL has attained great clinical attention as it prevents the bone erosion process in RA patients; however, it acts only on bone and exhibits no clinical benefits in controlling synovial tissue inflammation and cartilage destruction. Therefore, therapeutics that target many pro-inflammatory cytokines and effectively prevent synovial inflammation and bone destruction with minimal or no toxic regimen are greatly needed for RA patients.

Natural products have now been widely used worldwide as a complementary and alternative medicine to treat various disorders, including autoimmune diseases. The medicinal value of *Spirulina platensis* (Freitas et al., 2021), *Syzygium fruticosum* (Moni et al., 2021), *Lepidagathis hyaline* (Fahad et al., 2021), *Aglaonema hookerianum* (Goni et al., 2021), *Caesalpinia ferrea* (Macedo et al., 2020), *Amburana cearensis* (Silva et al., 2020), *Rhamnus triquetra* (Iqbal et al., 2020) has been recently at the forefront. Various medicinal plants possess bioactive components like furazan-3 amine (Khan et al. 2020), andrographolide (Hossain et al. 2021), and bromelain (Chakraborty et al. 2021) with anti-microbial, neuro-modulatory, anti-oxidant, anti-thrombolytic, and anti-cancer pharmacological properties. For instance, emodin has been evaluated for its therapeutic efficacy against tumor growth in lung carcinoma (Akkol et al. 2021a, b). Also, coumarin, furanocoumarins, and other coumarin-associated compounds help overcome the side effects and drug resistance of chemotherapeutic agents and possess high anti-cancer activities (Ahmed et al. 2020; Akkol et al. 2020). Furthermore, salvinorin A has been demonstrated to strongly inhibit ovalbumin-induced airway hyperreactivity (Rosi et al. 2017). Most importantly, terpineol exhibited a neuroprotective effect via modulation of dopamine receptor D2 in an inflammatory animal model of depression (Vieira et al. 2020). Unlike terpineol, several other natural compounds like African oil palm are used to treat neurological disorders (Akkol et al. 2021a, b; Islam et al. 2021). While, the anti-nociceptive and anti-inflammatory activity of Ophiorrhizarugosa rugose have been ascribed in various painful settings (Uddin et al. 2021). Notably, the adverse effects of prescribed drug–food interactions, especially for COVID-19,

have highlighted the medical importance of natural compounds in treating several inflammatory diseases (Agagunduz et al. 2021). A National Centre of Complementary and Integrative Health (NCCIH) pilot study found that the conventional gold standard drug, methotrexate, and ayurvedic treatments were similarly efficacious for RA. Indian traditional medicinal systems, particularly the Unani system, include several naturally derived herbal formulations that have long been recommended in the treatment of RA. UNIM-301, a polyherbal Unani formulation administered via oral gavage, exhibited intense anti-arthritic activity via modulating the expression levels of TNF-a, IL-6, and IL-1β in an adjuvant-induced rat arthritic model. Also, the same report has negated the toxic side effects associated with chronic and long-term use of UNIM-301 (Singh et al. 2015).

Moreover, our previous report has demonstrated an anti-arthritic efficacy of an aqueous suspension of Majoon Ushba via altering NF-κB and MAPKs pathway in fibroblast-like synoviocyte (FLS) cells obtained from adjuvant-induced arthritic (AA) rats (Ganesan et al. 2016). Majoon Chobchini (MC) is a polyherbal Unani compound that has been used holistically in India to treat RA. However, its scientific validation and underlying therapeutic mechanism in RA have still not been elucidated. Notably, NCCIH/National Institutes of Health (NIH) future strategic plans have strongly emphasized exploratory efforts in unraveling the therapeutic mechanism of action of Unani products for its scientific validation in clinical settings. Therefore, the current investigation aimed to identify and propose a scientific molecular basis for the therapeutic intervention of Majoon Chobchini in RA.

# Materials and methods

## Chemicals and reagents

Complete Freund's adjuvant (CFA), methotrexate, and TRAP staining kit were both procured from Sigma-Aldrich (St. Louis. MO). ELISA analysis kits for genes TNF-α, IL-1β, IL-6, and IL-17 were bought from PeproTech (Rocky Hill, USA). Dulbecco's modified Eagle's medium (DMEM) along with fetal bovine serum (FBS) and antibiotic solution were all obtained from Gibco BRL (Grand Island, NY, USA). FITC-conjugated monoclonal CD90.2 antibody was purchased from BioLegend (San Diego, CA, USA). JAK-1, p-JAK-1, JAK-3, p-JAK-3, STAT-3, p-STAT-3, RANKL, OPG primary antibodies were purchased from ABclonal (Woburn, MA, USA), and secondary antibodies conjugated with HRP and FITC were obtained from Cell Signaling Technology (Beverly, MA, USA). 4′, 6-diamidino-2-phenylindole (DAPI) was obtained from Thermo Fischer Scientific (Waltham, Massachusetts, USA). All other reagents

and solvents for experimental use were of analytical standard procured from local commercial sources.

## Animals

Wistar Albino experimental rats of 150–180 g (either sex) were obtained from the Animal House Facility of the School of Biosciences and Technology (SBST), Vellore Institute of Technology (VIT), Tamil Nadu, India. All experimental animals were kept in an Institutional animal house and were made acclimatized to conventional housing conditions of $25 \pm 2$ °C with a 45–55% humidified atmosphere and 12-h light–dark cycle. Experimental rats were allowed free access to commercial food and sterilized water ad libitum. The animal experiments and protocols were endorsed by the Institutional Animal Ethical Committee (IAEC), Vellore Institute of Technology India (VIT/IAEC/15/Sep2/28; dated Sep 2, 2018) and followed the guidelines of the Committee for the Purpose of Control and Supervision on Experiments on Animals (CPCSEA), India.

## Drug and dosage

Majoon Chobchini was purchased from the National Institute of Unani Medicine (NIUM), Bangalore, India. The drug is processed via blending functional herbal parts of 10 various plants of medicinal value (Table 1), as mentioned in the Indian Unani Pharmacopoeia, Part-II, Volume I by Ministry of AYUSH, Government of India. Briefly, Majoon Chobchini (100 g) was dissolved in sterile milli-Q water and extracted using ultrasonication for an hour at room temperature. The semi-solid extract of Majoon Chobchini was then collected, and the contents were dried under reduced pressure using a rotary evaporator, lyophilized, and stored at − 20 °C for further downstream use. In the preliminary dose-finding study, a homogeneous aqueous suspension of Majoon Chobchini was prepared in 1% phosphate-buffered saline, and arthritic rats were treated with increasing concentrations of Majoon Chobchini (250, 500, 750, and 1000 mg).

A significant reduction in paw swelling and inflammation was observed in 500–1000 mg/kg b wt doses of Majoon Chobchini. These two therapeutic dosages were selected for further experiments. However, the dried extract of Majoon Chobchini was suspended in a cell culture medium and sterile filtered before the in vitro experiments. Methotrexate (MTX), a gold standard anti-arthritic care medicine at 1 mg/kg b wt dosage, was used as a reference drug based on the previous reports.

## Establishment of arthritis and treatment protocol

Arthritis was established in the experimental rats according to the previously published procedure (Ganesan et al. 2016). In brief, experimental rats were intradermally administered with 0.1 ml CFA (per ml paraffin oil containing 10 mg of heat-killed *M. tuberculosis*) into the right hind foot of rats on day 0. Following adjuvant injection, the rats were randomly caged into six groups ($n = 6$ per group). Group A: non-arthritic rats received no administration or treatment. Group B: adjuvant-induced arthritic (AA) control rats received CFA. Group C and Group D contain AA rats orally administered with aqueous suspensions of Majoon Chobchini at 500 and 1000 mg/kg b wt, respectively. Group E: AA rats were injected intraperitoneally with the standard drug methotrexate (1 mg/kg b wt). The Majoon Chobchini or reference standard drug methotrexate treatment was initiated on day 11 when the clinical signs of arthritis peaked. The treatment was given one time daily for 10 days, i.e., 11th to 20th day. After the completion of treatments and post-radiographic assessment, the rats were subjected to the euthanasia method of sacrifice, and serum was separated for analysis. Hind limbs were aseptically separated and fixed in a 10% formalin.

## Physical measurement of arthritis

The elevation of arthritis severity was measured every 2 days by two independent observers post adjuvant induction.

**Table 1** Medicinal plant ingredients of Majoon Chobchini

| SL. no. | Unani name | Scientific name | Parts used | Weight in g (g) |
|---------|------------|-----------------|------------|-----------------|
| 1 | Chobchini | *Smilax china* Linn | Rhizome | 250 |
| 2 | Khusyat-us-Salab | *Orchis mascula* Linn | Tuber | 50 |
| 3 | Khulanjan | *Alpinia galanga* Willd | Rhizome | 40 |
| 4 | Gul-e-Gaozaban | *Borago officinalis* Linn | Flower | 25 |
| 5 | Behman Safaid | *Centaurea behen* Linn | Root | 25 |
| 6 | Behman Surkh | *Salvia haematodes* Linn | Root | 25 |
| 7 | Shaqaq-ul-Misri | *Pastinaca secacul* Linn | Rhizome | 25 |
| 8 | Abresham | *Bombyx mori* Moth., | Silk cocoon | 15 |
| 9 | Mughas | *Litsea chinensis* Lam | Bark | 15 |
| 10 | Jadwar | *Delphinium denudatum* Wall | Tuber | 10 |

The substantial changes in body weight and degree of paw edema were scored via a widely used grading system, in a blinded fashion, based on a scale of 0–4: 0 = absence of inflammation; 1 = possible inflammation and redness of the digit; 2 = moderate inflammation and redness; 3 = severe inflammation and redness of the limb and 4 = most severe inflammation, redness, physical deformity and disability of the limb. Bodyweight and paw edema were assessed using weighing balance and Vernier caliper, respectively. Pre-induction values for body weight and paw edema were measured just before arthritis induction and were considered as a baseline for assessing the physical changes on subsequent days.

For radiographic images of the hind limbs of experimental rats, the following protocol was performed on day 21 prior to sacrifice under anesthesia. The images were processed using X-ray MBR-1505R (Hitachi Medical Corporation, Japan) apparatus and film (Fuji Film, Tokyo, Japan). Rats were placed with a focal distance of 60 cm below the X-ray source operated at 5 mA with 40 kV and exposed for about 1 s. The severity of the joint deformity was certified on a large scale of 0–4 according to the extent of joint space and changes in joint structure by two observers not informed of the experimental conditions.

## Hot plate test

The anti-nociceptive activity of Majoon Chobchini on experimental rats was measured using a hot plate test. Rats were centrally placed on a hot plate enclosed with four plexiglass walls and maintained at a stable temperature of 55 °C. The reaction time taken for either to start paw licking or jumping was recorded. The rats were withdrawn from the plate immediately post licking a hind paw or with the absence of response occurred within 30 s. The drug was orally administered 30 min before performing the procedure, and the experiment was carried out three times in an interval of 5 min duration.

## Histopathology analysis

Post fixation with 10% neutral-buffered formalin, the excised rat hind limb was decalcified using 10% EDTA solution. Then, the decalcified joint specimen was subjected to dehydration using different graded series of alcohol. Following paraffin embedding, the knee joints were sectioned coronally (5 μm) and stained with hematoxylin and eosin dye (7 min). Next, the sections were washed with distilled water for 10 min for morphological evaluation. Further, separate sections were stained with safranin O (0.1% for 5 min) to assess the integrity of cartilage tissue. The stained tissue sections were focused under a microscope for evaluating cellular infiltration, joint space, pannus thickness, and cartilage

degradation with slight modification. Staining intensity was assessed for three sections per sample under blinded condition by two individual pathologists on a semi-quantitative scale of five-point (0 = absent, 1 = weak inflammation, 2 = mild inflammation, 3 = severe inflammation, and 4 = very severe inflammation).

## Estimation of reactive oxygen species (ROS)

Detection of ROS expression levels in the synovial tissues of experimental rats was assessed using 2, 7-dichlorofluorescein diacetate (DCFDA) fluorescent dye. Briefly, homogenized synovial tissues from the respective experimental groups were treated with DCFDA (10 μM) at 37 °C for 1 h. Post ice-cold phosphate-buffered saline (PBS) wash, the ROS levels were quantified using a fluorescence spectrophotometer (F-7000 FL Spectrophotometer) via estimating the release of fluorescent DCF with an excitation wavelength (488 nm) and an emission wavelength (510 nm).

## Western blot analysis

Total proteins from synovial tissues of experimental groups and isolated cells were extracted using RIPA lysis buffer (Sigma, USA) consisting cocktail of protease and phosphatase inhibitor. Following protein estimation via the Bradford method (Bio-Rad, Hercules, CA, USA), the lysates with 30 μg protein per lane were separated in 10% SDS-PAGE and electrotransferred onto membranes (polyvinylidene difluoride) (Amersham Pharmacia Biotech, Uppsala, Sweden). Next, membranes containing separated proteins were incubated with 5% BSA overnight at 4°C and then subsequently probed with primary antibodies targeted against JAK-1 (total), p-JAK-1, JAK-3 (total), p-JAK-3, STAT-3 (total), p-STAT-3, RANKL levels, and OPG for overnight at 4 °C. After the respective primary antibody incubation, primary antibodies were reacted with HRP-labelled secondary antibodies for two h at 37 °C. The protein bands were imaged using enhanced chemiluminescence (ECL) solution (Millipore, USA), and immunoreactive bands were developed in autoradiography film. β-Actin was considered a loading control, and the relative protein expression was calculated using software ImageJ version 1.48 (Wayne Rasband, Maryland U.S.).

## Estimation of cytokine production

The concentration of cytokine (TNF-α, IL-6, IL-17, and IL-1β) levels was estimated in the serum samples of experimental rats using commercial ELISA kits (PeproTech, NJ, USA). The optical density (OD) values for the samples were taken at 405 nm wavelength with a correction wavelength of

630 nm using a BioTek microplate reader (BioTek, Hercules, CA, USA).

## Quantitative real-time polymerase chain reaction (qRT-PCR) analysis

Post extraction using TRIzol reagent (Sigma Aldrich, St. Louis, USA) and purity check, the isolated total RNA was quantified using Nanodrop (Nanodrop Technologies, Wilmington, DE, USA). The synthesis of cDNA using a higher-capacity cDNA reverse transcription 326kit (Applied Biosystems, CA, USA) was carried out. Quantitative PCR was then performed using the Eva-Green Supermix PCR kit (Bio-Rad, Hercules, CA, USA) onto the manufacturer's protocol. The designed primer sequences are shown in Table 2. Amplification was performed under the cycling parameters: 95 °C (15 min), 94 °C (15 s), 40 cycles of 60 °C (30 s), and 72 °C (30 s) using C1000 Touch PCR detection instrument (Bio-Rad, Hercules, CA). GAPDH was used as an internal control for normalization of the relative mRNA values of corresponding target genes, and the results were calculated using the $2^{-\Delta\Delta CT}$ comparative cycle threshold method.

## Immunohistochemistry

For deparaffinization, knee joint tissue sections were passed through xylene solutions and rehydrated with graded alcohol series. The sections were blocked for peroxidase activity using 0.3% hydrogen peroxide in methanol for 20 min and then blocked at 37 °C for one hour with BSA (5%). After incubation with primary anti-rat iNOS and anti-rat COX-2 antibodies overnight at 4 °C, the sections were then reacted with HRP-conjugated secondary antibody for another 30 min at room temperature. Next, the antibody interaction was detected with DAB (3, 3-diaminobenzidine) substrate. Tissue sections were carefully counterstained using hematoxylin. Post staining, sections were again dehydrated to be permanently fixed for microscopy analysis. The stained sections were further captured under the Olympus photomicroscope (Tokyo, Japan).

## Isolation of bone marrow monocyte-macrophage

Bone marrow monocyte-macrophage cells (BMMs) were obtained, as mentioned previously (Ganesan and Rasool 2019). Briefly, rat hind legs were separated at the hip joint, with intact femur region. After the clearance of excess joint tissue muscle, both ends of the femur region were removed sterile, and a needle (25-G) with complete cell culture DMEM medium was used to remove the bone marrow onto a sterile culture plate. The collected cells were seeded for 12 h in DMEM medium supplemented with 10% FBS and 1% antibiotic–anti-mycotic solution. Following completion of incubation, non-adherent cells were pelleted and resuspended further in a complete DMEM cell culture medium. Lastly, cells were cultured in 60 mm tissue culture dishes in the presence of M-CSF (macrophage colony-stimulating factor) (25 ng/ml) concentration for consecutive 3 days.

## Isolation and primary culture of fibroblast-like synoviocytes cells

At the peak episode of arthritis, the hind paws of AA rats were surgically removed, and synovial joint tissues were procured under a sterile condition. Subsequently, freshly isolated synovial tissues were minced with type II collagenase (0.4%) prepared in DMEM supplemented with 5% FBS incubated at 37 °C for 4 h. The isolated cells were then cultured in DMEM medium supplemented with 10% FBS and 1% antibiotic–anti-mycotic solution and incubated at 37 °C for cells to properly adhere. Post incubation overnight, the non-adherent synovial cells floating in the culture medium were replaced with freshly prepared complete DMEM media. The cultured cells were then immediately passaged upon 90% confluency and used for downstream experiments.

**Table 2** Primer sequences

| | Sequences of the primer pairs used for qRT-PCR | |
|---|---|---|
| TNF-a | 5'-GGCATGGATCTCAAAGACAACC -3' | 5 '-AAATCGGCTGACGGTGTGG-3 ' |
| IL-6 | 5' -TACCACTTCACAAGTCGGAGG-3 ' | 5 '-CAATCAGAATTGCCATTGCACAAC-3 ' |
| IL-1β | 5' -TCTCACAGCAGCATCTCGAC-3 ' | 5 '-GGTCTCATCATCCCACGAG-3 ' |
| IL-17 | 5' -TCCAGAAGGCCCTCAGACTACC-3 ' | 5 '-AGGCTCCCTCTTCAGGACCAG-3 ' |
| COX-2 | 5' -CTCTTCCGAGCTGTGCTGC-3 ' | 5 '-TGTGTTTGGGGTGGGCTTC-3 ' |
| iNOS | 5' -GGCTACCAGATGCCCGATG-3 ' | 5 '-CCACTCGTACTTGGGATGCTC-3 ' |
| RANKL | 5' -CCGAGACTACGGCAAGTACC -3' | 5 '-CTGCGCTCGAAAGTACAGGA-3 ' |
| OPG | 5 '-ACAGTTTGCCTGGGACCAAA-3 ' | 5 '-TC ACAGAGGTCAATGTCTTGGA-3 ' |

## FLS characterization and treatment

The synovial FLS cells on passage 4 were processed for phenotypic characterization by staining with FITC-conjugated CD90.2 monoclonal antibody as described previously (Ganesan and Rasool 2019). Briefly, isolated cells were stained with FLS cell surface CD 90.2 marker and analyzed using FACS caliber system (BD Biosciences, New Jersey, USA). These cells were further passaged and used for subsequent experiments. For treatment, control FLS cells were left untreated. AA-FLS cells were incubated with or without Majoon Chobchini (200 and 300 µM) or methotrexate (1 µg/ml) for 24 h.

## TRAP analysis

For osteoclast differentiation, AA-FLS-treated/untreated cells were co-cultured with BMMs in quantity tissue culture plates described previously (Ganesan and Rasool 2019). Following differentiation, TRAP analysis was carried out using a TRAP staining acid phosphatase kit (Sigma Aldrich; St. Louis, MO). The TRAP staining solution was then removed, cells were rinsed in PBS and fixed for 15 min with formaldehyde solution (4%) at room temperature. The cells that were found TRAP-positive and contained ≥ 3 nuclei were focused under an inverted Olympus microscope and were considered as matured osteoclasts. The number of formed osteoclasts per experimental group was the value averaged from the triplicates performed in the experiment.

## Bone resorptive assay

Following AA-FLS treatment, cells were co-cultured with rat BMMs on a 24-well Corning Osteo-Assay surface plate (Corning Life Sciences, MA, USA) made up of a smooth surface that mimics bone mineral composition. Post 7-day incubation, the culture medium was carefully aspirated, and the cells were smoothly removed using 100 µl of bleach solution (10%) incubated at room temperature for 5 min. Following the bleaching process, the plate was rinsed in PBS and air-dried for about 3–5 h for photographs of the resorption area formed by the functional matured osteoclasts using an inverted Olympus microscope (Olympus, Tokyo, Japan) (magnification 40×).

## Immunofluorescence staining analysis

FLS cells were seeded onto glass coverslips (gelatin-coated) for fluorescence staining and placed in a six-well tissue culture plate. The attached cells were fixed using paraformaldehyde (4%) solution, permeabilized with Triton X-100 (0.2%) solution for 5 min, and blocked with incubation in BSA (5%) for 30 min at room temperature. The coverslips were

suspended in primary anti-p-STAT-3 antibodies overnight at 4 °C. STAT-3 expression was detected using FITC-tagged secondary antibody upon incubation at room temperature for 2 h. Cell nuclei were then visualized with 4′6-diamindino-2-phenylindole (DAPI; 1 µg/ml) (Sigma-Aldrich, St Louis, MO, USA) for 5 min and fluorescent-stained images were photographed using fluorescence microscopy (Olympus America, Melville, NY, USA).

## Liquid chromatography–Mass spectrometry (LC–MS) analysis of Majoon Chobchini

The LC–MS analysis of Majoon Chobchini was determined using Dionex Ultimate 3000 micro-LC fitted with C18, 150 × 4–6 mm, and 5 µm reversed-phase column (Thermo Fisher Scientific, Waltham, MA, USA). The mobile phase used was water and acetonitrile at a constant flow rate of 200 µl/min. Initially, the sample was mixed in a 1:1 ratio of acetonitrile and methanol. Next, the mixture was then vortexed and sonicated. The prepared sample was diluted at 1:10 times, after which the samples were mixed in the mobile phase, and 40 µl was injected into the LC–MS column for analysis. The mass spectra were generated at 70 eV electron impact ionization energy with a mass range ($m/z$ 40–500) at a rate of 0.5 scan/s. The bioactive constituents of Majoon Chobchini were pinpointed via comparison of the retention time (RT) and generated mass spectra of each separated peak with reference spectra to the LC/MS data bank.

## Acute toxicity study of Majoon Chobchini

The acute toxicity study of Majoon Chobchini was in accordance with the Organization for Economic Cooperation and Development (OECD) guidelines for the testing of chemicals—420. To minimize the use of animals, a limit test at a single oral dose of 2000 mg/kg b wt. Majoon Chobchini was performed using female Wistar albino rats ($n = 5$ per group; 150–180 g). In parallel, five experimental rats were given no treatment to establish a comparative normal control group. All experimental rats were observed periodically for initial 24 h and then once per day for continuous 14 days (Traesel et al. 2014).

## Sub-acute toxicity determination of Majoon Chobchini

For evaluation of repeated 28-day toxicity of Majoon Chobchini, the animals were randomly divided into three experimental groups ($n = 10$/group; five males and five females in each group). Group I received no treatment and served as a negative control. Group II was administered orally daily once with 1000 mg/kg b wt. of Majoon Chobchini for 28

**Fig. 1** LC–MS chromatogram of Majoon Chobchini. Representative chromatograms of Majoon Chobchini (MC) for identification of bioactive compounds at RT **A** 4.1 min **B** 14.1 min **C** 25.2 min **D** 30.4 min. *LC–MS* Liquid Chromatography–Mass Spectroscopy ▶

consecutive days. Group III (satellite group) received a maximum dose of 1500 mg/kg b wt. of Majoon Chobchini for 28 days and were then scheduled for follow-up examinations for the next 14 days. The doses selected were in accordance with the OECD guideline—407 (28 days—repeated dose oral toxicity study). During the period of treatment, body weight, food, and water intake and clinical examination for the possible signs of toxicity were assessed once daily.

Post treatment, all experimental animals were sacrificed, and blood samples were collected for examining various hematological parameters as described previously (Traesel et al. 2014). Also, biochemical analysis for the markers of renal activity (blood urea, creatinine, and bilirubin), liver (alanine aminotransferase and aspartate aminotransferase), and other parameters like albumin and cholesterol were performed using a commercially available kit (Roche).

Furthermore, the vital organs (kidney, liver, spleen) were weighed and fixed in buffered formalin (10%). Post fixation, samples were paraffin-embedded, sectioned (5 µm), and stained with hematoxylin and eosin to be examined under a light microscope for histological parameters like degeneration, congestion, necrosis, extravasation of blood, and fibrosis.

## Statistical analysis

The statistical calculation was determined with SPSS windows version 15.0 (Cary, NC). The experimental data were presented as mean $\pm$ SEM (standard error of the mean). The significant difference between control and treatment groups was determined by one-way analysis of variance (ANOVA) with the help of Bonferroni multiple comparison post test. At $p$ values < 0.05, the data were considered statistically significant.

## Results

### Reckoning the bioactive components of Majoon Chobchini

The majority of herbal medicines are reservoirs of bioactive compounds that provide pharmacological benefits. In this study, the phytochemical screening for the presence of bioactive compounds in Majoon Chobchini was performed using LCMS analysis. The LC chromatogram of Majoon
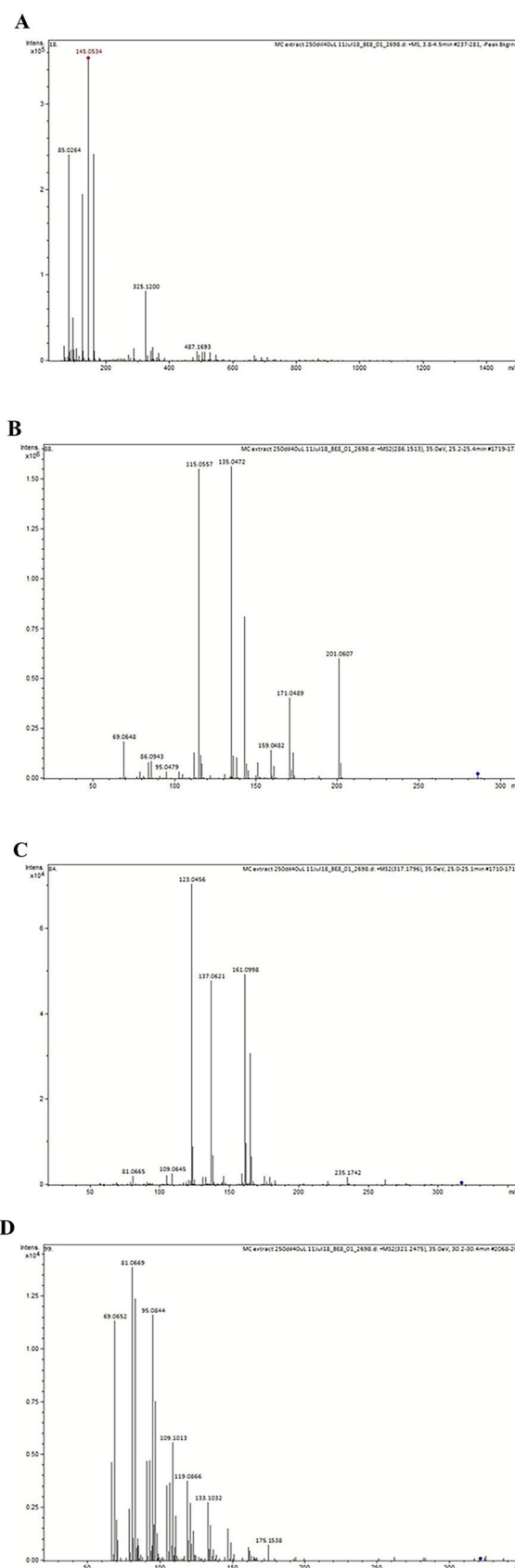
**Table 3** Bioactive components of MC from LCMS data

| SL. no. | Parent mass | Score | Compound |
|---------|-------------|-------|----------|
| 1 | 286.1513 | 0.7660 | Piperine |
| 2 | 145.0534 | 0.666 | Dimethylfumarate (fumaric acid) |
| 3 | 325.1200 | 0.28663 0.31142 0.34753 | Mahaleboside Phaseolidin Glabridin |
| 4 | 487.1693 | 0.39265 0.37848 | Pyranocyanin Linalool |
| 5 | 317.1796 | 0.2965 0.24745 0.56059 0.51370 0.4424 0.4422 | Pollenitin Homoferreirin Gingerol Calendic acid Nordihydrocapsiate Perilloside |
| 6 | 611.3570 | 0.5052 0.5050 0.4683 0.4462 0.4332 0.0109 0.0496 | Delphinidin 3 rhamnoside 5 glucoside Quercetin 3 galactoside Hesperidin Cyanidin 3 glucogalactoside Cyanidin 3 gentiobioside Liensinine Endomorphin I |
| 7 | 454.2832 | 0.3465 | Colupox A |
| 8 | 595.1672 | 0.3718 0.3053 0.2716 0.3503 0.4691 0.3579 0.3380 | Scoporin xyloside Epigallocatechin Gallocatechin Gravebioside Isorientin 6 rhamnoside Cyanidin 3 rhamnoside 5 glucoside Cyanidin 3 rutinoside |
| 9 | 69.0292 | 0.4167 | Hydroxypropionic Acid |
| 10 | 69.0648 | 0.4163 | Hydroxypropionic acid |
| 11 | 115.0557 | 0.4316 0.4225 | Hydroxypropionic acid Pterin |
| 12 | 135.0472 | 0.4123 0.3766 0.2857 | Hydroxybutyric acid Polyglutamic acid Pyrrolidone carboxylic acid |
| 15 | 159.0482 | 0.1851 0.1782 | Dimethyl 5 heptenol 2 Ethly 2 heptenol |
| 16 | 171.0489 | 0.3652 | Cichorigenin |
| 17 | 201.0607 | 0.4736 | 3 Methyl 2 phenylbutanol |
| 18 | 123.0456 | 0.4444 | Barbituric acid |
| 19 | 161.0998 | 0.2930 0.3632 | Triden penatyne Ketogluaramic acid |
| 20 | 235.1742 | 0.17527 0.15723 | Trimethoxycinnamate Trimethoxycinnamic acid |
| 21 | 69.0652 | 0.413 | Hydroxypropionic acid |
| 22 | 133.1032 | 0.3766 0.2857 | Polyglutamic acid Pyrrolidone carboxylic acid |
| 23 | 175.1538 | 0.3154 | Cichorigenin (Asculetin) |

Chobchini was shown in Fig. 1. The major bioactive chemical components of Majoon Chobchini were obtained by comparing corresponding LC chromatogram peaks retention time with mass spectra of LC–MS data bank. LC–MS analysis showed the presence of various bioactive chemical components in Majoon Chobchini (Table 3).

## Majoon Chobchini attenuates the development of arthritis in the AA model

The onset of the arthritis disease severity is phenotypically marked by a decrease in body weight and pronounced paw swelling. We, therefore, explored whether Majoon Chobchini exhibited anti-arthritic efficacy via restoration of body

weight and decrease in paw swelling in the CFA-induced arthritis (AA) model of RA. The development of arthritis was at its peak on day 11 post single intradermal injection of CFA. The in vivo treatment schema for the experimental animals is represented in Fig. 2A. However, oral administration of Majoon Chobchini in AA rats diminished paw swelling and induced a normal increase in body weight compared to AA control rats (Fig. 2B–D). Notably, high-dose treatment of Majoon Chobchini (1000 mg/kg b wt) was more effective

in diminishing paw swelling and improving body weight gain than 500 mg/kg b wt dose in AA rats (Fig. 2B–D). A similar reduction in paw swelling and increased body weight was demonstrated in AA rats treated with MTX (1 mg/kg b wt) (Fig. 2B–D).

The disease progression of arthritis is also manifested by nociceptive behavior and joint pathological changes like massive cellular infiltration, reduced joint space, pannus formation, and cartilage degradation. In
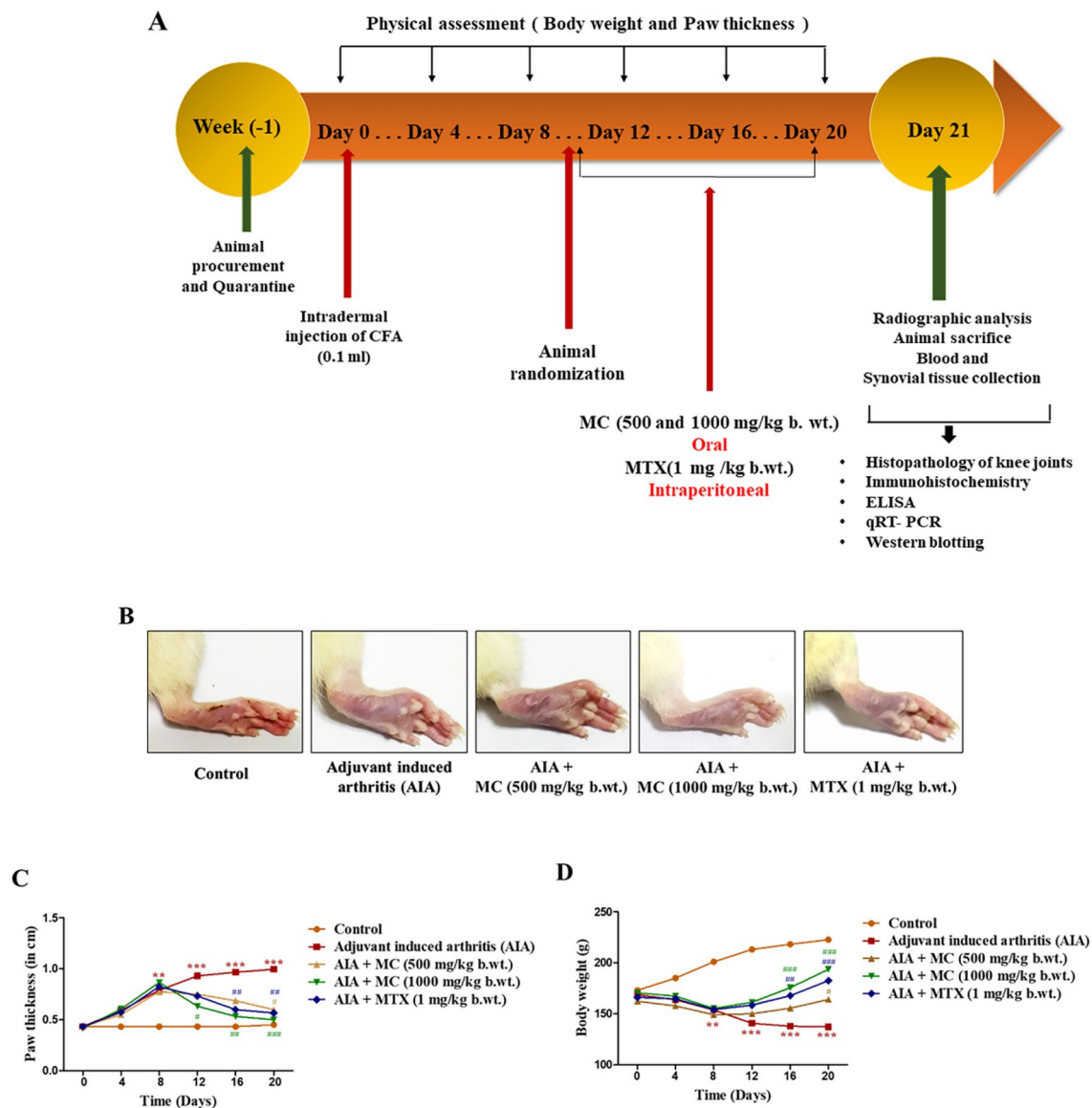


**Fig. 2** Effect of Majoon Chobchini (MC) treatment in CFA-induced arthritic (AA) rats in vivo. Rats were injected with CFA into the right hind foot on day 0. MC and MTX were orally administered once daily from day 11 to day 20. **A** Experimental timeline indicating in vivo arthritic induction and treatment schedule of Majoon Chobchini (MC). **B** Photographs of representative macroscopic paw images on day 21 and assessment of physical changes, such as **C** paw thickness and **D** alterations in body weight, were assessed. **E** Anti-nociceptive activity of Majoon Chobchini (MC) in experimental rats. **F** Representative images of H & E stained knee joints in experimental rats for pathological changes like cellular infiltration, joint space and pannus formation (Original Magnification × 100 and × 400). Black double arrow: joint space and red arrow: pannus formation. All error bars represent mean ± SEM. ***$p < 0.001$ vs control. ###$p < 0.001$, ##$p < 0.01$ and #$p < 0.05$ vs AA rats. *CFA* Complete Freund's adjuvant, *SEM* standard error of mean
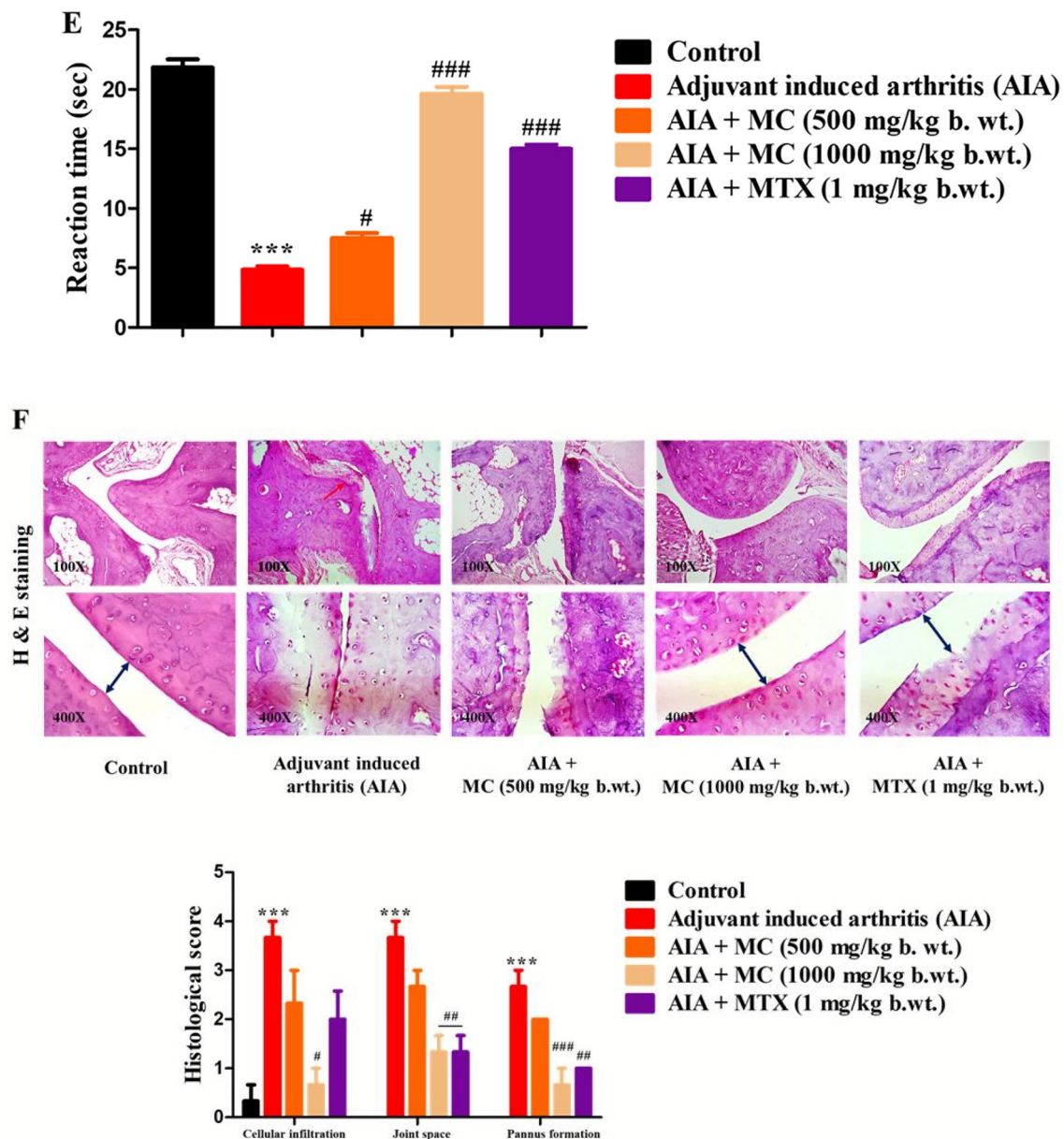
**Fig. 2** (continued)

the present study, the anti-nociceptive phenomena of Majoon Chobchini were evaluated via a hot plate test. As shown in Fig. 2E, the response time of AA rats to nociception was dramatically reduced in comparison to normal rats. Whereas treatment of AA rats with Majoon Chobchini (1000 mg/kg b wt) or methotrexate (1 mg/kg b wt) showed better analgesic activity as determined by an increase in response time (Fig. 2E). However, the effect of Majoon Chobchini on joint pathological changes was evaluated via histological studies. In histological examination, knee joints of AA rats showed severe joint space narrowing, mass infiltration of immune cells, and pannus formation (Fig. 2F). Importantly, normal joint space, attenuated immune cell infiltration, and pannus structure were examined in AA rats administered with Majoon Chobchini at 1000 mg/kg b wt dose (Fig. 2F).
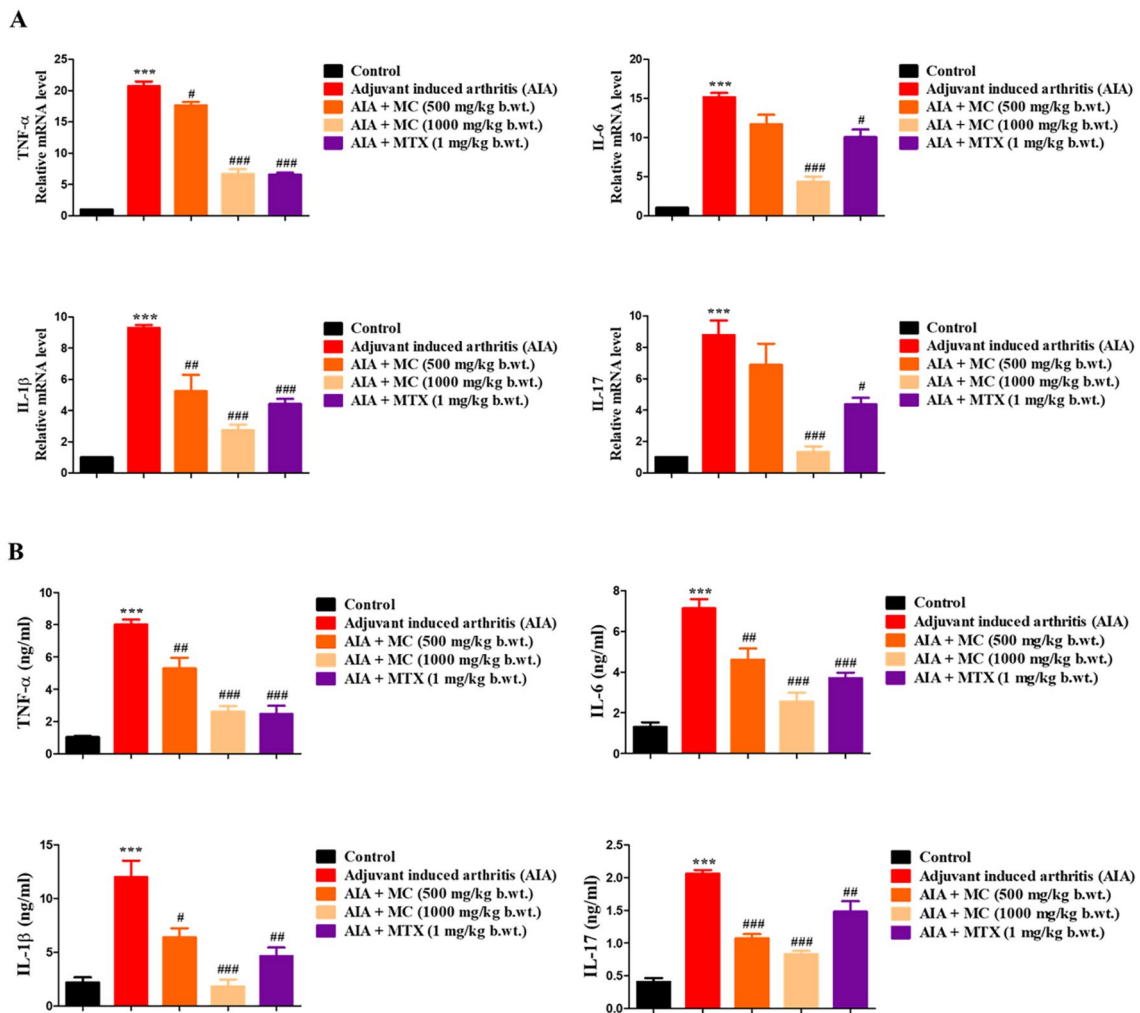
**Fig. 3** Effect of Majoon Chobchini (MC) on the cytokine over-production in AA rats. **A** The q-RT-PCR analysis was performed to measure the expression of TNF-α, IL-1β, IL-6, and IL-17 in the synovial tissues of AA rats. **B** The protein levels of TNF-α, IL-6, IL-1β and IL-17 were assessed in the serum samples of experimental rats by ELISA. All error bars depict mean ± SEM of three independent experiments. ***$p < 0.001$ vs control. ###$p < 0.001$, ##$p < 0.01$ and #$p < 0.05$ vs AA rats. *TNF* tumor necrosis factor, *IL* interleukin, *AA* adjuvant-induced arthritis

## Majoon Chobchini ameliorates pro-inflammatory cytokines expression in AA rats

Pro-inflammatory mediators are known to favor the development and progression of arthritis. Thus, we studied the effect of Majoon Chobchini on the expression of pro-inflammatory mediators, such as TNF-α, IL-6, IL-1β, and IL-17, in AA rats. As shown in Fig. 3A, B, we found significantly higher expression of TNF-α, IL-6, IL-1β and IL-17, in the synovial tissue at the mRNA level and in the serum at protein level, in AA rats in comparison to its expression levels in normal rats. In contrast, administering a higher dose of Majoon Chobchini (1000 mg/

kg b wt) markedly decreased pro-inflammatory cytokine protein and mRNA expression levels in AA rats (Fig. 3A, B). Altered protein and mRNA expression of TNF-α, IL-6, IL-1β, and IL-17 were also observed in AA rats that were administered with MTX (1 mg/kg b wt) (Fig. 3A, B). Cumulatively, these results documented that Majoon Chobchini inhibited the production of critical pro-inflammatory cytokines that mainly contributes to immune cell influx and synovial tissue inflammation pertaining to the disease severity of RA.
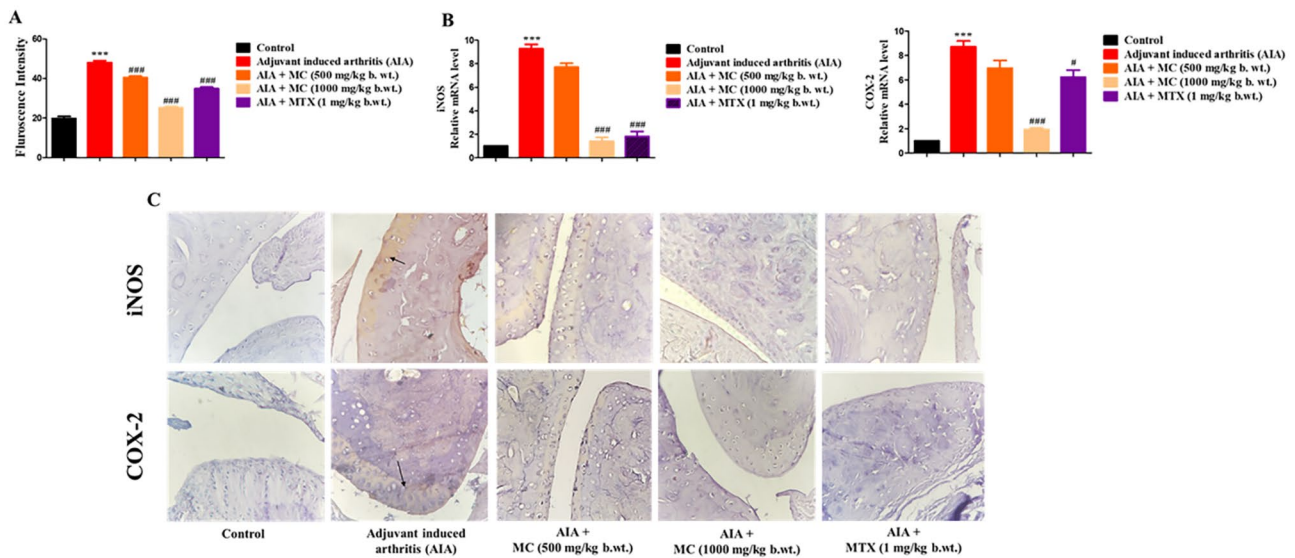
Springer

**Fig. 4** Effect of Majoon Chobchini (MC) on the intracellular free-radical formation. **A** The level of free radicals in the synovial joint tissue of AA rats was evaluated by the DCFH-DA method. Fluorescence intensity units (FIU) are shown as means ± SEM. **B** COX-2 and iNOS levels were quantified by qRT-PCR analysis. **C** Synovial tissue expression of COX-2 and iNOS were analyzed via immuno-histochemical analysis (Magnification × 100). All error bars depict mean ± SEM ($n = 3$ independent experiments were performed). ***$p < 0.001$ vs control. ###$p < 0.001$, ##$p < 0.01$ and #$p < 0.05$ vs AA rats. *qRT-PCR* quantitative real-time polymerase chain reaction, *DCFH-DA* dichloro-dihydro-fluorescein diacetate, *COX* cyclooxygenase, *iNOS* inducible nitric oxide synthase

## Free radical scavenging activity of Majoon Chobchini in AA rats

Oxidative stress is often associated with the increased production of several pro-inflammatory mediators in RA. Excessive ROS level establishes oxidative stress environment, so we examined the effect of Majoon Chobchini on the level of free radicals in the synovial joint tissue of AA rats via the DCFH-DA method. As shown in Fig. 4A, increased ROS levels were observed in AA rats as detected with an enhanced release of fluorescent DCF. In contrast, a significant reduction in the level of ROS was marked in AA rats administered with Majoon Chobchini (1000 mg/kg b wt) as compared to AA rats (Fig. 4A).

## Majoon Chobchini downregulates COX-2 and iNOS expressions in synovial joint tissue of AA rats

Nitric oxide synthase (iNOS) and cyclooxygenase 2 (COX-2) enzymes are mainly responsible for overshooting the production of nitric oxide and pro-inflammatory mediators in RA. The inhibitory efficacy of Majoon Chobchini on the expression of the enzymes iNOS and COX-2 was investigated in AA rats, and Majoon Chobchini-treated AA rats. As shown in Fig. 4B and C, a remarkable up-regulation in the mRNA level and protein expression of COX-2 and iNOS was observed in the synovial joint tissue of AA rats in comparison to normal rats. Intriguingly, Majoon Chobchini

administration to AA rats reversed the increased expression of iNOS and COX-2 in a dose-wise manner as compared to AA rats (Fig. 4B, C).

## Majoon Chobchini inhibits cartilage destruction and bone erosion in AA rats

The formation of destructive proliferative tissue pannus and pro-inflammatory mediators further invades cartilage that results in bone erosion in the disease progression of RA. To test the protective ability of Majoon Chobchini against damage of synovial joint cartilage, safranin O staining analysis was performed on the excised knee joints of experimental rats. As shown in Fig. 5A, synovial tissue of AA rats exhibited low staining intensity for safranin O, indicating loss of proteoglycans and degraded cartilage lining compared to normal rats. In contrast, oral treatment of Majoon Chobchini abrogated cartilage degradation in AA rats as determined by intense safranin O staining (Fig. 5A). In contrast, methotrexate (1 mg/kg b wt) treatment did not restore the cartilage damage observed in AA rats (Fig. 5A).

Cartilage damage and bone loss, in turn, lead to irreversible joint deformity. Therefore, radiographic analysis was carried out to evaluate the reduction in joint deformity in the experimental rats. The radiographical assessment depicted bone morphological changes in AA rats. (Fig. 5B) Whereas Majoon Chobchini treatment at the dose of 1000 mg/kg b.wt in AA rats prevented bone erosion or joint deformity in a
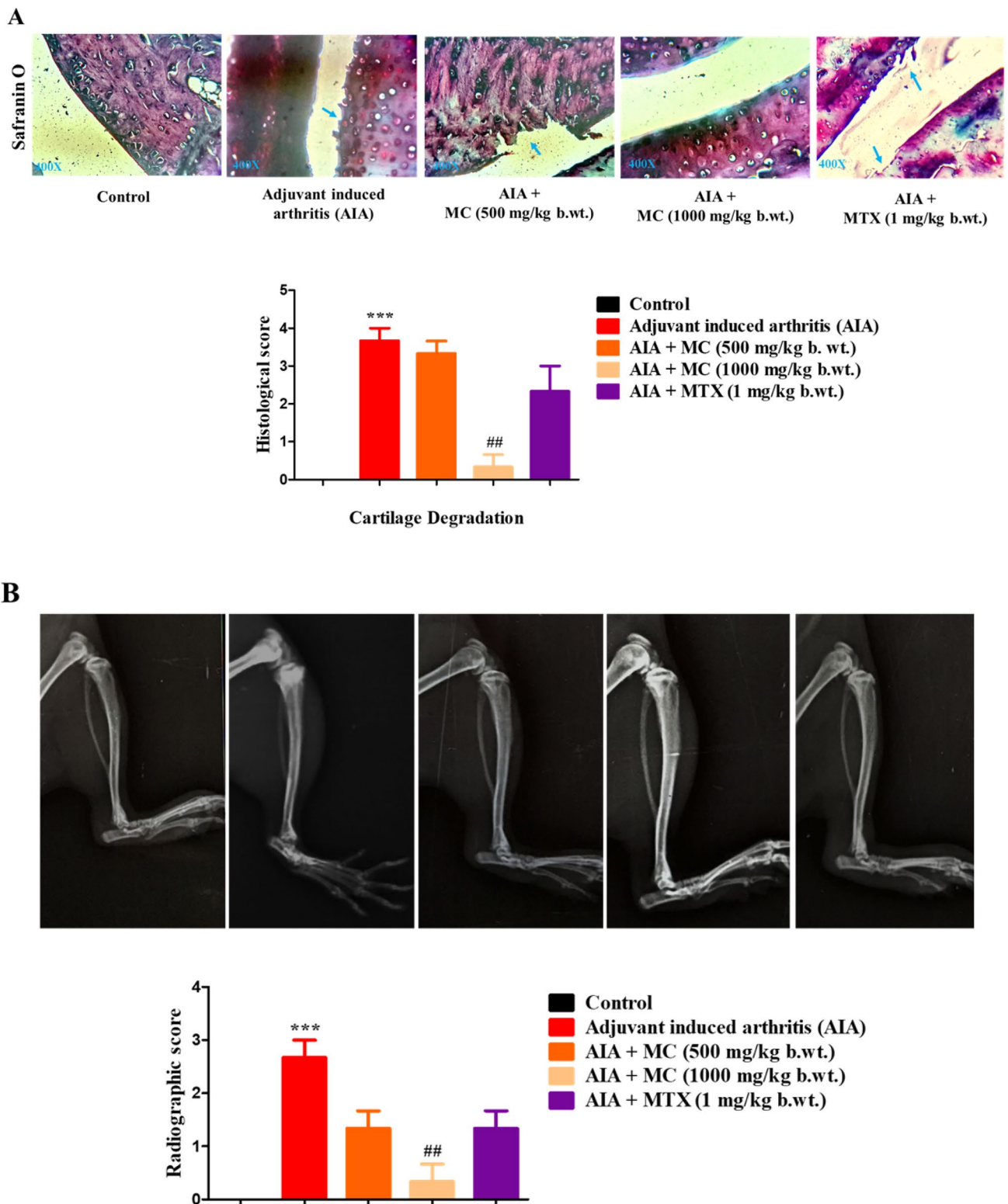
**Fig. 5** Effect of Majoon Chobchini (MC) on cartilage degradation and joint deformity in AA rats. **A** Representative images of safranin O-stained synovial tissue joints depicting cartilage degradation. Blue arrow: cartilage degradation. **B** Radiographic scanning images of rat joints and radiographical scoring based on a semi-quantitative scale in a blinded fashion
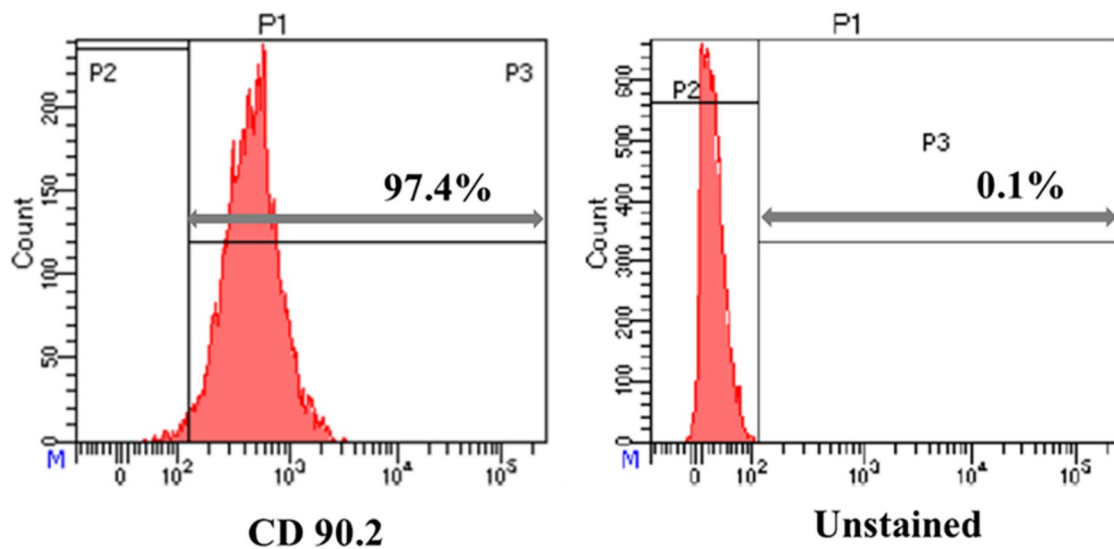
**Fig. 6** The purity check of FLS cells at the fourth passage was evaluated via FACS analysis using FITC-tagged antibody to cell surface CD 90.2 marker. Left panel, unstained cells, Right panel, > than 97% of FLS cells were stained positive for CD 90.2. *FLS* fibroblast-like synoviocytes, *FACS* fluorescence-activated cell sorting, *CD* cluster differentiation

dose-dependent manner (Fig. 5B). Methotrexate exhibited no therapeutic effect on bone damage in AA rats.

## Majoon Chobchini impairs osteoclast formation and resorption

Dysregulated osteoclast formation delineated by the acquisition of phenotypic marker TRAP is an essential pathological event in the bone destruction process of RA. In this study, we elucidated the effect of Majoon Chobchini on osteoclast formation in a co-culture model, AA-FLS cells, and BMMs and in the joint tissue sections of experimental animals. Of note, 97% of isolated cells stained positive for CD 90.2 cell surface marker (Fig. 6). Again, MTT assay revealed that Majoon Chobchini treatment with 200 and 300 μM concentrations was used for in vitro experiments as it showed no marked reduction in cell viability of AA-FLS cells until 24 h (Online Resource 1). As evidenced from TRAP staining results, a significant increase in the formation of TRAP$^+$ multi-nucleated osteoclast cells was obtained upon co-culture of BMMs with untreated AA-FLS cells (Fig. 7A). In contrast, treatment with Majoon Chobchini significantly reduced osteoclast formation in a concentration-dependent manner (Fig. 7A). Again, methotrexate treatment also reduced osteoclast formation (Fig. 7A).

Matured osteoclasts formed primarily facilitates bone resorption that leads to bone loss and reduced ambulation in RA. So, the efficacy of Majoon Chobchini against resorption of the mineralized bone surface was assessed using osteo assay plates. The multi-nucleated osteoclasts formed actively resorbed bone surface as evident from the increase in the number of resorption pits in group wherein BMMs were co-cultured with AA-FLS cells compared to BMMs cultured alone (Fig. 7B). Whereas Majoon Chobchini treatment dose-dependently mitigated the resorptive activity of osteoclasts (Fig. 7B). Collectively, these observations suggest that Majoon Chobchini attenuates osteoclast formation and its bone resorptive activity.

## Majoon Chobchini regulates osteoclastogenic factors expression in AA-FLS cells

Receptor activator of nuclear factor kappa-B ligand (RANKL) is an obligatory factor that requisites osteoclast differentiation. While, osteoprotegerin (OPG) binds to RANKL and inhibits osteoclast differentiation. To support the inhibited role of Majoon Chobchini on osteoclast cell formation and its resorption activity, the protein expressions of osteoimmunological molecules, such as RANKL and OPG, were investigated by western blotting analysis. AA-FLS cells were incubated with or without the increasing concentration of Majoon Chobchini or methotrexate. As shown in Fig. 7C, the increased expression of RANKL with a concurrent reduction in the expression of OPG was observed at the protein level in AA-FLS cells compared to normal FLS cells. Interestingly, the elevated expression level of OPG over reduced RANKL levels was observed in AA-FLS cells treated with Majoon Chobchini in a concentration-wise manner (Fig. 7C).

## Majoon Chobchini influences JAK-dependent STAT signaling pathway in AA rats

The key signaling molecule JAKs and the downstream transcription factor STATs are critically involved in RA's inflammation and synovial joint destruction process. To explore whether JAK/STAT signaling cascade underlies the anti-arthritic and anti-osteoclastogenic efficacy of Majoon Chobchini in RA, we investigated its phosphorylated level in the synovial joint tissue of AA, and Majoon Chobchini-treated AA rats. An increased level of phosphorylated JAK1-Tyr1034/1035 and phosphorylated JAK3-Tyr 980/981 proteins was observed in the synovial joint tissue of AA rats in comparison to normal rats (Fig. 8A). In addition, an increased phosphorylated

level of STAT-3 protein was observed in the synovial joint tissue of AA rats (Fig. 8A). As shown in Fig. 8A, Majoon Chobchini administration markedly downregulated the level of phosphorylated JAK1-Tyr1034/1035, JAK3-Tyr980/981, and phosphorylated STAT-3 proteins in the synovial joint tissue of AA rats. Notably, methotrexate treatment also abrogated JAK/STAT signaling activation in AA rats compared to that of AA control rats (Fig. 8A).

Furthermore, Majoon Chobchini efficacy on the phosphorylation of STAT-3 in AA-FLS cells was elucidated in vitro. Immunofluorescence analysis showed an increased cellular expression level of the activated STAT-3 transcription factor in AA-FLS cells (Fig. 8B). Otherwise, Majoon Chobchini treatment resulted in the
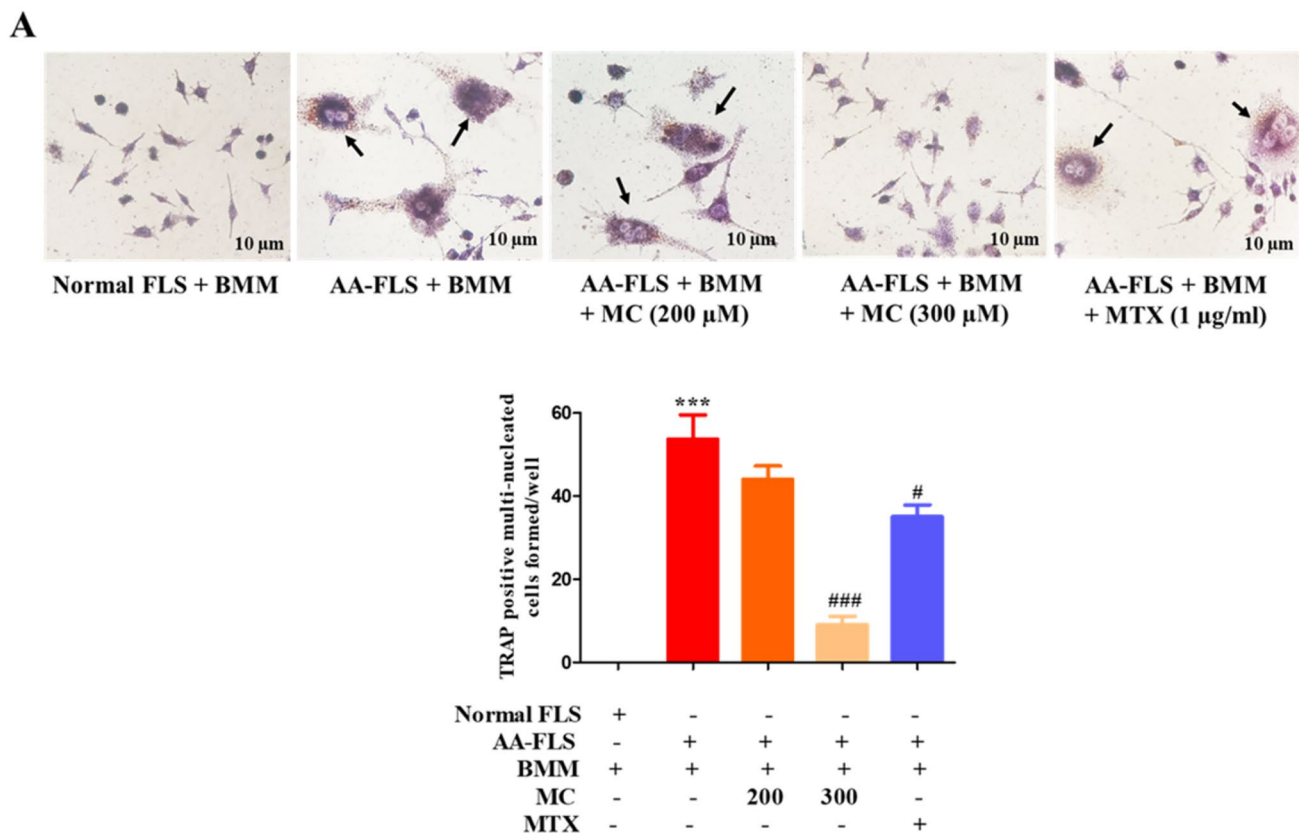


**Fig. 7** Effect of Majoon Chobchini (MC) on the osteoclastogenic inducing potential of AA-FLS. Rat bone marrow monocyte/macrophage cells were co-cultured with normal FLS or AA-FLS, AA-FLS treated with Majoon Chobchini (MC) (200 and 300 μM), AA-FLS treated with MTX (1 μg/ml). **A** TRAP staining analysis was conducted to identify the generation of the multinucleated osteoclast cells. TRAP-positive cells that have three or more nuclei were counted as matured osteoclasts using an inverted Olympus microscope (magnification × 40). **B** Bone resorption assay was performed on osteo assay plate and resorption areas were imaged using

an inverted Olympus microscope. × 40 magnification. **C** The protein expression levels of RANKL and OPG molecules were analyzed using western blotting. The expression value of target proteins (RANKL and OPG) was determined as target protein/β-actin ratio. The result represents mean ± SEM ($n = 3$ individual experiments were performed). ***$p < 0.001$ vs normal FLS + BMM. ###$p < 0.001$, #$p < 0.01$ and #$p < 0.05$ vs AA-FLS + BMM. *MTX* Methotrexate, *TRAP* tartrate-resistant acid phosphatase, *RANKL* receptor activator of nuclear factor kappa-B ligand, *OPG* Osteoprotegerin
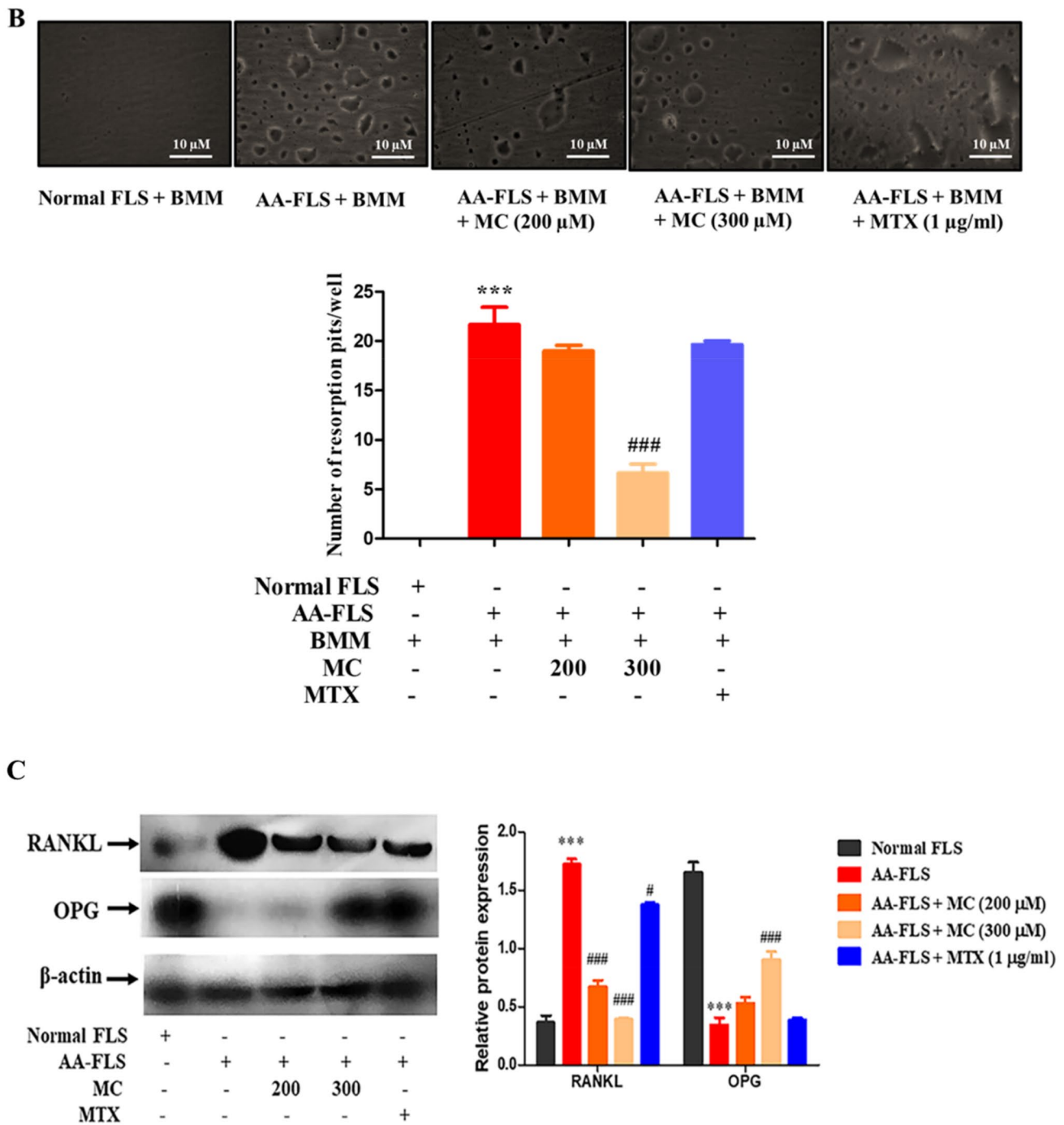
**B**



| Normal FLS + BMM | AA-FLS + BMM | AA-FLS + BMM + MC (200 µM) | AA-FLS + BMM + MC (300 µM) | AA-FLS + BMM + MTX (1 µg/ml) |



**C**



**Fig. 7** (continued)

hypo-phosphorylation of the STAT-3 transcription factor in AA-FLS cells in a concentration-wise manner (Fig. 8B).

### Effect of Majoon Chobchini on acute toxicity studies

Oral administration of Majoon Chobchini demonstrated no treatment-associated mortality throughout the study period. No pathological abnormalities or toxicity signs were observed in any animals. The body weight, food, and water intake also remained unchanged as compared to the untreated control
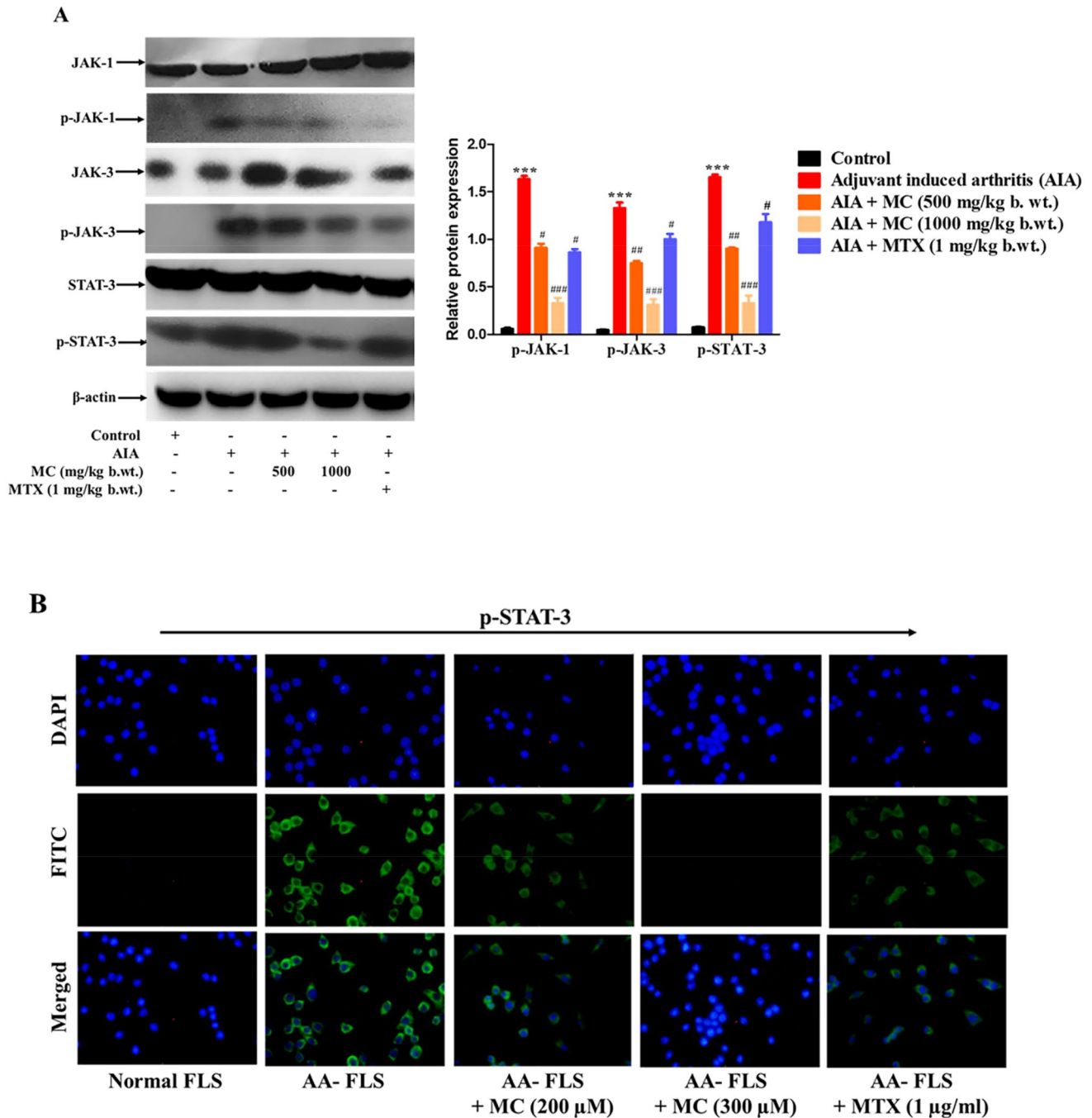
**Fig. 8** Effect of Majoon Chobchini (MC) on the JAK/STAT3 signaling cascade in AA-FLS and synovial tissues of AA rats. **A** Post sacrifice, the synovial tissues were isolated from experimental rats to analyze the level of JAK-1 (total), p-JAK-1, JAK-3 (total), p-JAK-3, STAT-3 (total) and p-STAT-3 using western blotting. The expression of phosphorylated proteins and total protein was normalized to β-actin loading control, followed by calculating phosphorylated protein/total protein ratio to determine the altered expression of phosphorylated target protein. **B** The altered expression of p-STAT-3 was analyzed via immunofluorescence staining analysis. All error bars depict mean ± SEM of three independent experiments. ***$p < 0.001$ vs control. ###$p < 0.001$, ##$p < 0.01$ and #$p < 0.05$ vs AA rats. ***$p < 0.001$ vs normal FLS. ###$p < 0.001$, ##$p < 0.01$ and #$p < 0.05$ vs AA-FLS. *JAKs* Janus Kinases, *STAT* signal transducer and activator of transcription

group (Data not shown). Therefore, it is considered that Majoon Chobchini is safe even at higher dose levels, and the oral LD$_{50}$ should be regarded as to be greater than 2000 mg/kg b. wt in rats.

## Effect of Majoon Chobchini on sub-acute toxicity studies

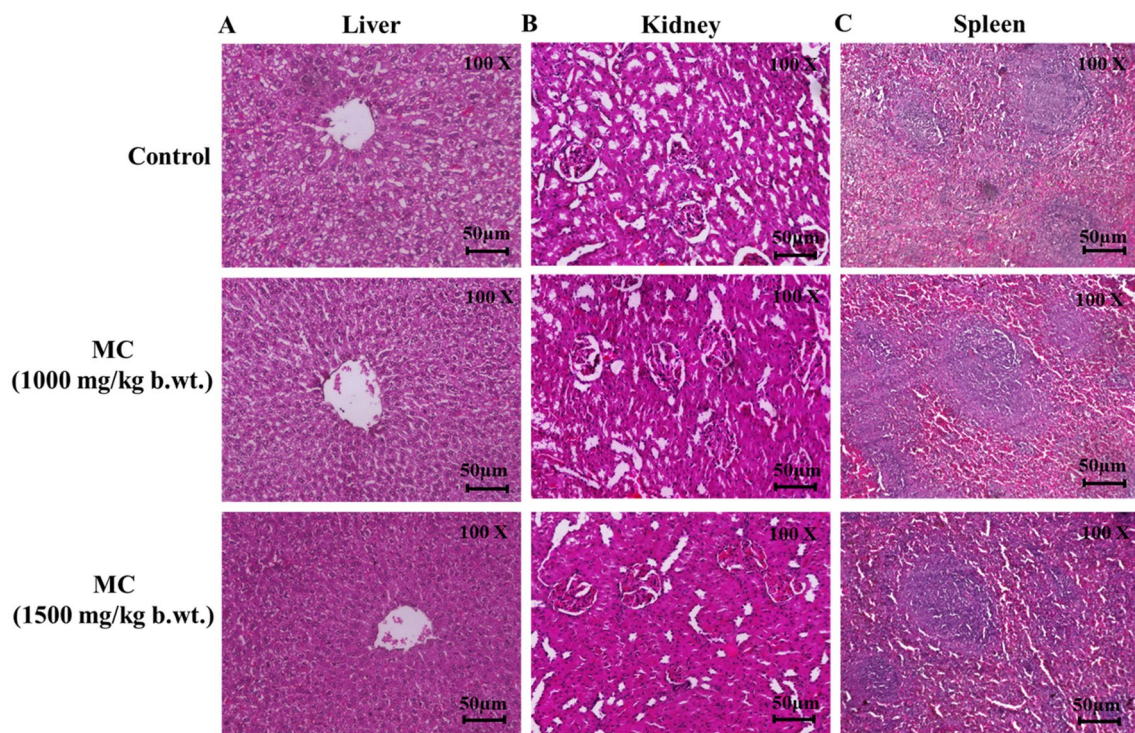In sub-acute administration of Majoon Chobchini, no signs

**Fig. 9** Effect of Majoon Chobchini on the vital organs in acute oral toxicity. Photographs of histopathological sections of **A** Liver **B** kidney **C** Spleen. Maginification: × 100; scale bar: 50 μm

of toxicity or changes in body weight (Online Resource 2), food and water consumption (Data not shown) were observed in the treated or satellite group compared to the untreated control group. All the experimental rats survived throughout the 28-day study period. No significant differences were observed in relative organ weights between the treated and control group (Online Resource 3). With respect to hematological (Data not shown) and biochemical parameters (Online Resource 4), no major differences were observed in treated groups compared to untreated control groups. Histology of vital organs showed no major alterations. The liver architecture exhibited a clear lumen of the central vein with no signs of lesions or necrosis (Fig. 9). No degeneration of glomeruli, proximal and distal tubules was observed in the kidney (Fig. 9). Cross-sectional observation of spleen tissues appeared normal (Fig. 9). However, there was mild congestion observed in both control and treated group that can be incidental and has no relation with Majoon Chobchini treatment.

## Discussion

In the present paper, we examined the anti-arthritic effects and mechanism of action of Majoon Chobchini, a polyherbal Unani compound, during the disease progression in adjuvant-induced arthritic (AA) rat model of RA. The results demonstrated that Majoon Chobchini treatment could significantly decrease paw swelling, synovial inflammation, and immune cell infiltration in the AA rat model. Further, Majoon Chobchini inhibited osteoclast formation and suppressed bone erosion via altering RANKL/OPG axis. Strikingly, the therapeutic effects of Majoon Chobchini were via modulation of JAK-dependent STAT-3 activation.

Synovial fibroblasts and infiltrating immune cells are majorly responsible for producing several pro-inflammatory cytokines that play an indispensable role in the disease progression/severity of RA. TNF-α and cytokine IL-1β are the principal cytokines in regulating inflammation via the production of chemokines, such as MCP-1 and RANTES (chemotactic mediators), from synovial macrophages and RA-FLS cells (Neog et al. 2017). TNF-α and IL-1β also aggravate osteoclast formation and concurrent bone erosion via inducing the expression of RANKL from synovial fibroblasts in RA (Wang et al. 2016). TNF-α alone exhibits a direct role in inhibiting FoxP3 + Treg cell-dependent autoimmune suppression; thus, highlighting its unfavorable role in RA. Intriguingly, IL-1β has a more influential role than TNF- α in inducing cartilage destruction in patients with RA. IL-6 is another key pro-inflammatory cytokine involved in the pathogenesis of RA. Blockade of IL-6/IL-6R signaling prevents

osteoclast-mediated bone erosion by inhibiting RANKL secretion in RA-FLS cells (Yoshitak et al. 2008). IL-6 critically drives the differentiation of pathogenic T cells and subdues the suppressive function of natural Treg cells. IL-17 is a canonical cytokine of pathogenic Th17 subtype CD4 + T cells. The pro-inflammatory cytokine IL-17A has a remarkable role in promoting RANKL expression from RA-FLS cells; wherein, blockade of IL-17/JAK/STAT-3 pathway diminished RANKL-mediated osteoclastogenesis in RA (Ganesan and Rasool 2019). Experimental evidence has also revealed that blockade of IL-17 action reduced the formation of B-cell germinal center in RA (Benedetti and Miossec 2014). In this study, Majoon Chobchini dramatically decreased the expression and serum levels of TNF-α, IL-6, IL-1β, and IL-17 in AA rats, suggesting its potential beneficial effects in controlling inflammation and thus ameliorating disease progression of RA.

Reactive oxygen species (ROS) have also been studied to be strongly responsible for RA's pathogenesis. Literature studies suggest that the overproduction of tissue enzymes, such as iNOS and COX-2, impairs anti-oxidant defense mechanisms and thus influences inflammation and joint damage in RA. Higher levels of ROS induce polyunsaturated fatty acids oxidation in the mitochondrial membrane of RA-FLSs (Malemud 2018). Of note, the present study results showed that Majoon Chobchini prevented free-radical production and neutralized oxidative stress environment via downregulating the expression of tissue enzymes iNOS and COX-2 in the synovial joint tissues of AA rats.

Destruction of cartilage and bone erosion of synovial joints are the central events in patients with an advanced stage of RA and are associated with poor clinical outcomes. Experimental evidence has demonstrated that functionally active osteoclasts are highly important for the bone erosion phenomenon in RA (Ganesan and Rasool 2019). While, RANKL secreted from RA-FLS cells favors osteoclast formation and associated bone degradation in RA. RAFLS cells and macrophages in the hyperplastic synovium also secrete extracellular matrix-degrading enzyme MMP-9 and contribute to cartilage degradation in RA patients (Neog et al. 2017). In this study, Majoon Chobchini, but not MTX, was able to inhibit cartilage destruction and bone erosion in AA rats. Importantly, Majoon Chobchini prevented osteoclast inducing the potential of AA-FLS cells, osteoclast formation from its precursor cells, and bone erosion. However, MTX treatment showed a minimal effect in the reduction of osteoclast formation but did not alleviate bone erosion in vitro. The results of the current study contradicted the previous reports that demonstrated MTX in slowing the joint destruction process in RA; it can thus be attributed to bioavailability, drug dose, treatment alone or in combination, and treatment duration (Kang 2019; Williams et al. 1996). These data suggest that Majoon Chobchini can be used as

an alternative treatment option for preventing joint destruction in RA.

JAK-STAT signaling activation has been identified as an important downstream event for the excess release of TNF-α, IL-6, and IL-17 cytokines in RA. Previous studies have reported that blockade of JAK/STAT activation altered synovial inflammation and indirectly affected osteoclast formation in RA. The clinical efficacy of small molecule JAK inhibitors, such as tofacitinib and baricitinib, on inhibiting synovitis and bone erosion was noted in RA settings (Shim et al. 2018). Therefore, JAK/STAT signaling pathway inhibition has been regarded as a new targeted therapeutic approach in controlling the disease severity of RA. The present study revealed that Majoon Chobchini decreased the activation of JAK1 and JAK3 and their downstream signaling molecule STAT-3 in the synovial joint tissue of AA rats. In addition, Majoon Chobchini was able to reduce the activation of STAT-3 in AA-FLS cells. These findings reveal the dramatic efficacy of Majoon Chobchini in modulating the JAK/STAT-3 signaling cascade to abrogate the pathological processes, including inflammation and joint destruction that underlie RA disease severity.

The molecular characterization of Majoon Chobchini to unravel the biologically active components will undoubtedly validate its anti-inflammatory, anti-oxidant, and anti-osteoclastogenic activities in an AA model of RA. Onto this, LC–MS screening of Majoon Chobchini indicated the presence of chemical compounds including piperine, fumaric acid, gingerol, perilloside, quercetin 3 galactoside, hesperidin, cyanidin 3 glucogalactoside, cyanidin 3 gentiobioside, liensinine, epigallocatechin, gallocatechin, gravebioside, cyanidin 3 rhamnoside 5 glucoside, cyanidin 3 rutioside, and cichorigenin. Crucial findings have reported several pharmacological properties, such as anti-cancer, anti-inflammatory, anti-oxidant, anti-diabetics, and immunomodulatory effects, of these naturally derived compounds (Ganesan et al. 2016). The previous study has demonstrated that piperine suppressed IL-1β-induced production of MMP13, IL-6, COX-2, and activator protein 1 (AP-1) in RA patient-derived FLS cells (Bang et al. 2009). Gingerol displays its anti-inflammatory effects via significant inhibition of NK-kB and MAPK pathway activation. Besides, gingerol reduces COX-2 and iNOS expression in LPS-induced macrophages (Van Breemen et al. 2011). Anti-inflammatory, anti-arthritic, and free-radical scavenging activities have been established previously for fumaric acid, quercetin, and epigallocatechin (Shakya et al. 2014; Gardi et al. 2015; Karatas et al. 2019). In addition, cyanidin has been shown to interfere with IL-17-dependent activation of STAT-3 and inhibit osteoclast formation (Samarpita et al. 2020). Therefore, the anti-arthritic potential of Majoon Chobchini observed in this study might be ascribed to be mediated by its bioactive components.

In the present study, the LD$_{50}$ of Majoon Chobchini was found to be above 2000 mg/kg b wt in rats. Repeated dose study of Majoon Chobchini also demonstrated no pathological alteration, thus engendering it to be a safer alternative disease-modifying drug in the treatment of RA.

## Conclusion

In conclusion, the results presented in this study demonstrate that Majoon Chobchini ameliorated synovial inflammation, cartilage tissue degradation, and bone erosion in an AA rat model. Majoon Chobchini downregulated the expression of pro-inflammatory mediators, tissue enzymes (iNOS and COX-2), and altered free-radical levels in the AA rat model. In addition, Majoon Chobchini has a profound ability to inhibit osteoclast formation via altering RANKL/OPG axis and bone degradation. Significantly, Majoon Chobchini modulated JAK-dependent STAT-3 activation in the AA rat model and AA-FLS cells. Above all, Majoon Chobchini exhibited no toxic effects or pathological changes on its long-term administration. Collectively, this study, for the first time, scientifically proves the anti-inflammatory and anti-arthritic properties of Majoon Chobchini and its underlying molecular mechanism in RA, thus speculating it to be a frontline safer therapy in the management of RA.

**Supplementary Information** The online version contains supplementary material available at https://doi.org/10.1007/s13205-021-02985-4.

## Declarations

**Conflict of interest** The authors reported no potential conflict of interest.

**Data availability** The data of this article will be available upon request.

## References

Agagunduz D, Celik MN, Daziroglu MEC, Capasso R (2021) Emergent drug and nutrition interactions in COVID-19: a comprehensive narrative review. Nutrients 13(5):1550

Ahmed S, Khan H, Aschner M, Mirzae H, Akkol EK, Capasso R (2020) Anti-cancer potential of furanocoumarins: mechanistic and therapeutic aspects. Int J Mol Sci 21(16):5622. https://doi.org/10.3390/ijms21165622 (**PMID: 32781533; PMCID: PMC7460698**)

Akkol EK, Genc Y, Karpuz B, Sobarzo-Sanchez E, Capasso R (2020) Coumarins and coumarins-related compounds in pharmacotherapy of cancer. Cancer (basel) 12(7):1959. https://doi.org/10.3390/cancers12071959 (**PMID: 32707666; PMCID: PMC7409047**)

Akkol EK, Tatti II, Karatoprak GS, Agar OT, Yucel C, Sobarzo-Sanchez E, Capasso R (2021a) Is emodin with anticancer effects completely innocent? Two sides of the coin. Cancers (basel) 13(11):2733. https://doi.org/10.3390/cancers13112733 (**PMID: 34073059**)

Akkol EK, Tatti II, Cankaya I, Seker Karatoprak G, Carpar E, Sobarzo-Sanchez E, Capasso R (2021b) Natural compounds as medical strategies in the prevention and treatment of psychiatric disorders seen in neurological disease. Front Pharmacol 13(12):669638. https://doi.org/10.3389/fphar.2021.669638 (**PMID:34054540;PMCID:PMC8155682**)

Bang JS, Choi HM, Sur BJ, Lim SJ, Kim JY, Yang HI, Kim KS (2009) Anti-inflammatory and anti-arthritic effects of piperine in human interleukin 1β-stimulated fibroblast-like synoviocytes and in rat arthritis models. Arthritis Res Ther 11(2):R49

Benedetti G, Miossec P (2014) Interleukin 17 contributes to the chronicity of inflammatory diseases such as rheumatoid arthritis. Eur J Immunol 44(2):339–347

Chakraborty AJ, Mitra S, Tallei TE, Tareq AM, Nainu F, Cicia D, Dhama K, Emran TB, Simal-Ganada J, Capasso R (2021) Bromelain a potential bioactive compound: a comprehensive overview from a pharmacological perspective. Life (basel) 11(4):317

Fahad FI, Barua N, Islam MS, Sayem SAJ, Barua K, Uddin MJ, Chy MNU, Adnan M, Islam MN, Sayeed MA, Emran TB, Simal-Gandara J, Pagano E, Capasso R (2021) Investigation of the pharmacological properties of *Lepidagathis hyaline* nees through experimental approches. Life (basel) 11(3):180 (**PMID: 33668978;PMCID:PMC7996513**)

Freitas MA, Vasconcelos A, Goncalves ECD, Ferrarini EG, Vieira GB, Cicia D, Cola M, Capasso R, Dutra RC (2021) Involvement of opiod system and TRPM8/TRPA1 channels in the antinociceptive effect of *Spirulina platensis*. Biomolecules 11(4):592. https://doi.org/10.3390/biom11040592

Ganesan R, Rasool M (2019) Ferulic acid inhibits interleukin 17-dependent expression of nodal pathogenic mediators in fibroblast-like synoviocytes of rheumatoid arthritis. J Cell Biochem 120(2):1878–1893

Ganesan R, Doss HM, Rasool M (2016) Majoon ushba, a polyherbal compound ameliorates rheumatoid arthritis via regulating inflammatory and bone remodeling markers in rats. Cytokine 77:115–126

Gardi C, Bauerova K, Stringa B, Kuncirova V, Slovak L, Ponist S, Drafi F, Bezakova L, Tedesco I, Acquaviva A, Bilotto S (2015) Quercetin reduced inflammation and increased antioxidant defense in rat adjuvant arthritis. Arch Biochem Biophys 583:150–157

Goni O, Khan MF, Rahman M, Hasan MZ, Kader FB, Sazzad N, Sakib MA, Romano B, Haque MA, Capasso R (2021) Pharmacological insights on the antidepressant, anxiolytic and aphrodisiac potentials of *Aglanema hookerianum* Schott. J Ethnopharmacol 268:113664. https://doi.org/10.1016/j.jep.2020.113664.Epub (**PMID: 33278545**)

Hossain S, Urbi Z, Karuniawati H, Mohiuddin RB, Moh Qrimida A, Allzrag AMM, Ming LC, Pagano E, Capasso R (2021) *Andrographis paniculata* (Burm.f.) wall. ex Nees. An updated review of phytochemistry, antimicrobial pharmacology, and clinical safety and efficacy. Life (basel) 11(4):348

Hyrich KL, Inman RD (2001) Infectious agents in chronic rheumatic diseases. Curr Opin Rheumatol 13(4):300–304

Iqbal J, Abbasi BA, Ahmad R, Mahmoodi M, Munir A, Zahra SA, Shahbaz A, Shaukat M, Kanwal S, Uddin S, Mahmood T, Capasso R (2020) Phtogenic synthesis of nickel oxide nanoparticles (NiO) using fresh leaves extract of *Rhamnus triquetra* (Wall) and investigation of its multiple in vitro biological potentials. Biomedicines 8(5):117

Islam N, Khan MF, Nur S, Hanif NB, Kulsum U, Arshad L, Lyzu C, Cacciola NA, Capasso R, Haque MA (2021) Neuropharmacological insights of African oil palm leaf through experimental assessment in rodent behavioral model and computer-aided mechanism. Food Biosci 40:100881

Jaswal S, Mehta HC, Sood AK, Kaur J (2003) Anti-oxidant status in rheumatoid arthritis and role of anti-oxidant therapy. Clin Chim Acta 338(1–2):123–129

Jung SM, Kim KW, Yang CW, Park SH, Ju JH (2014) Cytokine-mediated bone destruction in rheumatoid arthritis. J Immunol Res 2014:263625

Kang JS (2019) Effects of methotrexate on collagen-induced arthritis in male Wistar rats. J Biomed Res 33(4):244

Karatas A, Dagli AF, Orhan C, Gencoglu H, Ozgen M, Sahin N, Sahin K, Koca SS (2019) Epigallocatechin 3-gallate attenuates arthritis by regulating Nrf2, HO-1, and cytokine levels in an experimental arthritis model. Biotechnol Appl Biochem. https://doi.org/10.1002/bab.1860

Khan MF, Kader FB, Arman M, Ahmed S, Lyzu C, Sakib SA, Tanzil SM, Zim AFMIU, Imran MAS, Venneri T, Romano B, Haque MA, Capasso R (2020) Pharmacological insights and prediction of lead bioactive isolates of Dita bark through experimental and computer-aided mechanism. Biomed Pharmacother 131:110774

Luo Q, Sun Y, Liu W, Qian C, Jin B, Tao F, Gu Y, Wu X, Shen Y, Xu Q (2013) A novel disease-modifying anti-rheumatic drug, iguratimod, ameliorates murine arthritis by blocking IL-17 signaling, distinct from methotrexate and leflunomide. J Immunol 191(10):4969–4978

Macedo NS, Silveira ZS, Bezerra AH, Costa JGMD, Coutinho HDM, Romano B, Capasso R, Cunha FABD, da Silva MV (2020) *Caesalpinia ferrea C. Mart.* (Fabaceae) phytochemistry, ethnobotany, and bioactivities: a review. Molecules 25(17):3831. https://doi.org/10.3390/molecules25173831 (**PMID:32842529; PMCID:PMC7503918**)

Malemud CJ (2018) Pharmacologic interventions for preventing chondrocyte apoptosis in rheumatoid arthritis and osteoarthritis. Drug Discov Concepts Mark 45:77. https://doi.org/10.5772/intercho-pen.73174

McInnes IB, Schett G (2007) Cytokines in the pathogenesis of rheumatoid arthritis. Nat Rev Immunol 7(6):429–442

Moni JNR, Adnan M, Tareq AM, Kabir MI, Reza ASMA, Nasrin MS, Chowdhury KH, Sayem SAJ, Rahman MA, Alam AK, Alam SB, Sakib MA, Oh KK, Cho DH, Capasso R (2021) Therapeutic potentials of *Syzgium fructicosum* fruit (seed) reflected into an array of pharmacological assays and prospective receptors-mediated pathways. Life (basel) 11(2):155

Neog MK, Pragasam SJ, Krishnan M, Rasool M (2017) p-Coumaric acid, a dietary polyphenol ameliorates inflammation and curtails cartilage and bone erosion in the rheumatoid arthritis rat model. BioFactors 43(5):698–717

Rossi A, Caiazzo E, Bilancia R, Riemma MA, Pagano E, Cicala C, Ialenti A, Zjawiony JK, Izzo AA, Capasso R, Roviezzo F (2017) Salvinorin A inhibits airway hyperactivity induced by ovalbumin sensitization. Front Pharmacol 7:525

Samarpita S, Ganesan R, Rasool M (2020) Cyanidin prevents the hyperproliferative potential of fibroblast-like synoviocytes and disease progression via targeting IL-17A cytokine signalling in rheumatoid arthritis. Toxicol Appl Pharmacol 391:114917

Shakya A, Singh GK, Chatterjee SS, Kumar V (2014) Role of fumaric acid in anti-inflammatory and analgesic activities of a *Fumaria indica* extracts. J Intercult Ethnopharmacol 3(4):173

Shim JH, Stavre Z, Gravallese EM (2018) Bone loss in rheumatoid arthritis: basic mechanisms and clinical implications. Calcif Tissue Int 102(5):533–546

Silva JHCE, Ferreira RS, Pereira EP, Braga-de-Souza S, Almeida MMA, Santos CCD, Butt AM, Caiazzo E, Capasso R, Silva VDAD, Costa SL (2020) *Amburana cearensis*: pharmacological and neuroprotective effects of its compounds. Molecules 25(15):3394. https://doi.org/10.3390/molecules25153394

Singh S, Kumar R, Jain H, Gupta YK (2015) Anti-inflammatory and anti-arthritic activity of UNIM-301 (a polyherbal unani formulation) in Wistar rats. Pharmacognosy Res 7(2):188

Susan ES, Firestein GS (2004) Rheumatoid arthritis: regulation of synovial inflammation. Int J Biochem Cell Biol 36(3):372–378

Traesel GK, de Souza JC, de Barros AL, Souza MA, Schmitz WO, Muzzi RM, Oesterreich SA, Arena AC (2014) Acute and subacute (28 days) oral toxicity assessment of the oil extracted from *Acrocomia aculeata* pulp in rats. Food Chem Toxicol 74:320–325

Uddin CMN, Adnan M, Chowdhury MR, Pagano E, Kamal ATMM, Oh KK, Cho DH, Capasso R (2021) Central and peripheral pain intervention by Ophiorrhizarugosa leaves: potential underlying mechanism and insight into the role of pain modulators. J Ethnopharmacol 276:114182. https://doi.org/10.1016/j.jep.2021.114182

Van Breemen RB, Tao Y, Li W (2011) Cyclooxygenase-2 inhibitors in ginger (*Zingiber officinale*). Fitoterapia 82(1):38–43

Vieira G, Cavalli J, Goncalves ECD, Braga SFP, Ferreira RS, Santos ARS, Cola M, Raposo NRB, Capasso R, Dutra RC (2020) Antidepressant—like effect of terpineol in an inflammatory model of depression: involvement of the cannabinoid system and D2 dopamine receptor. Biomolecules 10(5):792

Wang S, Wang Y, Liu X, Guan L, Yu L, Zhang X (2016) Anti-inflammatory and anti-arthritic effects of taraxasterol on adjuvant-induced arthritis in rats. J Ethnopharmacol 187:42–48

Williams AS, Camilleri JP, Goodfellow RM, Williams BD (1996) A single intra-articular injection of liposomally conjugated methotrexate suppresses joint inflammation in rat antigen-induced arthritis. Rheumatol 35(8):719–724

Yoshitake F, Itoh S, Narita H, Ishihara K, Ebisu S (2008) Interleukin-6 directly inhibits osteoclast differentiation by suppressing receptor activator of NF-κB signaling pathways. J Biol Chem 283(17):11535–11540